

CBETA Technical Report

D. Trbojevic

September 2018

Collider Accelerator Department
Brookhaven National Laboratory

U.S. Department of Energy

USDOE Office of Science (SC), Nuclear Physics (NP) (SC-26)

Notice: This technical note has been authored by employees of Brookhaven Science Associates, LLC under Contract No. DE-SC0012704 with the U.S. Department of Energy. The publisher by accepting the technical note for publication acknowledges that the United States Government retains a non-exclusive, paid-up, irrevocable, world-wide license to publish or reproduce the published form of this technical note, or allow others to do so, for United States Government purposes.

DISCLAIMER

This report was prepared as an account of work sponsored by an agency of the United States Government. Neither the United States Government nor any agency thereof, nor any of their employees, nor any of their contractors, subcontractors, or their employees, makes any warranty, express or implied, or assumes any legal liability or responsibility for the accuracy, completeness, or any third party's use or the results of such use of any information, apparatus, product, or process disclosed, or represents that its use would not infringe privately owned rights. Reference herein to any specific commercial product, process, or service by trade name, trademark, manufacturer, or otherwise, does not necessarily constitute or imply its endorsement, recommendation, or favoring by the United States Government or any agency thereof or its contractors or subcontractors. The views and opinions of authors expressed herein do not necessarily state or reflect those of the United States Government or any agency thereof.

CBETA TECHNICAL REPORT

[CBETA NOTE # 31]

LIST OF CONTRIBUTORS

PI-D. TRBOJEVIC, PI-G. HOFFSTAETTER, S. BROOKS, C. GULLIFORD, A. BARTNIK, J. S. BERG,
G. MAHLER, J. TUOZZOLO, N. TSOPAS, S. TRABOCCI, W LOU, N. BANERJEE, J. BARLEY,
I. BAZAROV, I. BEN-ZVI, D. BURKE, J. CRITTENDEN, J. DOBBINS, R. GALLAGHER, B.
HELTSLEY, R. HULSART, J. JONES, D. JUSIC, R. KAPLAN, D. KELLIHER, V. KOSTROUN, B.
KUSKE, Y. LI, M. LIEPE, W. LOU, G. MAHLER, M. MCATEER, F. MÉOT, R. MICHNOFF,
M. MINTY, R. PATTERSON, S. PEGGS, V. PTITSYN, P. QUIGLEY, T. ROSER, D. SABOL,
D. SAGAN, J. SEARS, K. SMOLENSKI, E. SMITH, V. VESHCHEREVICH, J. VÖELKER, D. WIDGER

*Cornell University - CLASSE
Brookhaven National Laboratory
Collider Accelerator Department*

This document includes twelve sections related to the previous Fractional Arc Test (FAT), CBETA final installation plan which follows the milestones signed in the contract with the New York State Energy Development Authority (NYSERDA). In the second part we provide a plan for final installation, hardware and software preparation and the beam commissioning. Recently the National Academy of Sciences released a study of "An Assessment of U.S.-Based Electron Ion-Collider Science". ... "The principal goals of the study were to evaluate the significance of the science that would be enabled by the construction of an EIC, its benefits to U.S. leadership in nuclear physics, and the benefits to other fields of science of a U.S.-based EIC. Several presentations to the committee specifically addressed the challenges and necessary innovations in accelerator science needed for constructing an EIC capable of addressing the most important science questions"..."To reach the performance goals of the proposed EIC conceptual designs, a number of accelerator advances are required. Several of these advances are common to all EIC designs and include the following: advanced magnet designs, strong hadron beam cooling, **high current multi turn ERL technology**, crab cavity operation with hadron beams, the generation of polarized ^3He beams, and development and benchmarking of simulation tools. The successful implementation of an EIC requires the successful validation of these key concepts through high-fidelity simulations and demonstration experiments. The following subsections review these enabling technologies, the present state of the art, and required research and development to meet EIC facility specifications and realize EIC science: **Energy Recovery Linacs**. ...The ERLs required for electron cooling are at scales much larger than supported by present-day experience, so a number of accelerator physics and technology challenges still need to be overcome with focused R&D and great attention to detailed simulations. The challenges center around the following three major areas: 1. Achieving high electron source brightness; 2. Maintaining high beam brightness through the accelerator transport -beam dynamics of an unprecedented number of spatially superposed bunches in the SRF linacs; very precise phase and amplitude control; 3. Dealing with unprecedented beam currents in SRF linacs (halo mitigation, beam breakup instabilities, higher order mode dissipation). Many of these R&D issues are being investigated vigorously in dedicated test facilities under construction and commissioning in laboratories around the world. Specifically, the 4-pass Fixed Field Alternating Gradient R&D loop for eRHIC, see Box 4.2 **CBETA and Fixed Field Alternating Gradient Optics** for Electron Acceleration. it could illuminate key issues including multi-turn beam-breakup instability thresholds for proof of possible cavity designs, halo and mitigation, beam - ion effects, and operational challenges such as instrumentation and stability of multi-turn beams..."

The suggestions obtained in this report of the National Academy of Sciences emphasize importance of the CBETA project and provides important directions for the project goals.

In the history of linear fixed field alternating gradient structures CBETA is the third proof of principle so far. Properties comparisons of EMMA (Electron Model for Many Applications), ATF (Accelerator Test Facility) test with FFA and CBETA, compiled by Stephen Brooks, are shown in the next two Fig. 0.0.1 and in Table 0.0.1, respectfully.

CBETA incorporates already existing Cornell ERL high-power injector, Main Linac Cryostat - MLC, and beam stop. To demonstrate four passes up in energy and four passes down in energy through a single arc subsection consisting of FFA magnets with a common vacuum chamber. In order to properly inject into and extract from this FFA arc, splitter subsections are inserted between the MLC and the FFA arc. In the contract the CBETA team was to

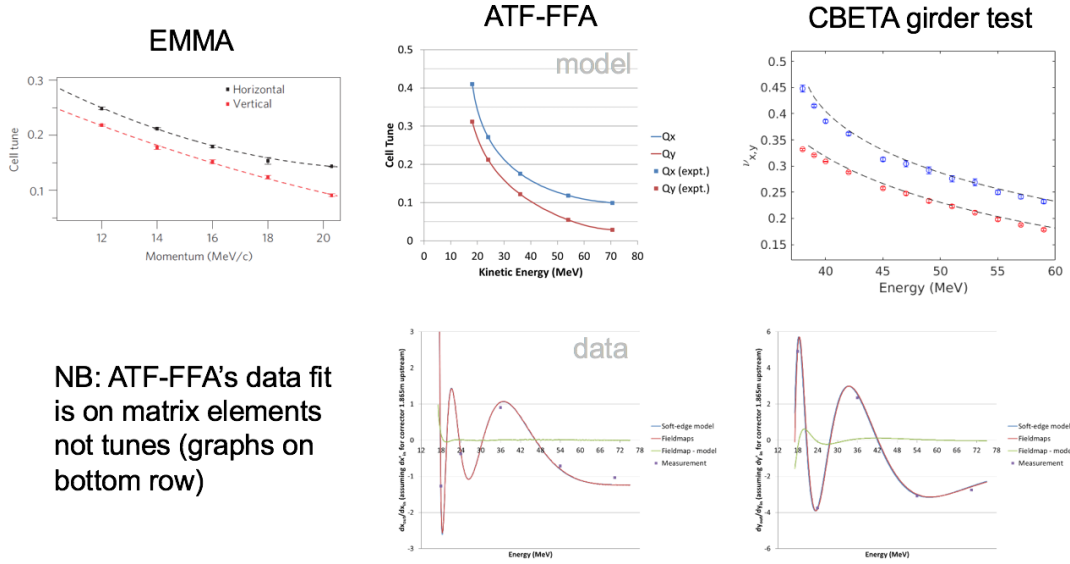


Figure 0.0.1: Results from all linear fixed field alternating gradient built so far.

Table 0.0.1: Linear Fixed Field Alternating Gradient EMMA-ATF-CBETA Comparison

Parameter	EMMA	ATF-FFA	CBETA girder	CBETA Future	Units
Energy Range	10-20	18-70.5	37.5-58.5	41.5-149.5	MeV k.e.
Momentum ratio	1.953	3.837	1.553	3.572	none
Radius of curv.	2.6372	2.01367	5.08787	5.08787	m
Eff. avg. dipole	0.0259	0.11761	(0.09834)	0.09834	T
Total angle	360	40	20	280	degrees
Operation mode	Storage ring	Transfer line	Transfer line	ERL	
Acceleration	Yes	None	None	Yes (linac)	
Lattice	Doublet	FODO	Doublet	Doublet	
Cell length	0.394524	0.234301	0.444	0.444	m
Cells per turn	42	54	72	107.5	
Length built	16.57	extrapolated 1.40581	extrapolated 1.776	racetrack 47.73	m

perform the fractional arc test and transport the beam through Main Linac Cryo-module and Prototype FFA girder in months of February, March, and April 2018. The deliverables are:

- A** -Pass the beam through the MLC, through one channel of one of the separator-combiners, and through an FFA arc girder.
- B** -Carry out performance testing of the identified sub-systems with and without the beam.
- C** -Document all trouble shooting incidents, performance issues and rectify them.

The second part of this document is related to the final period of the CBETA project: finalizing the construction and installation and begin commissioning. As mentioned above the major remaining milestones of the project are:

Task 7: Complete Girder Production Run - end of November 2018

Task 8: Complete Final Assembly and Pre-Beam Commissioning - end of February 2019

Task 9: Single Pass Beam Energy Scan - March to June 2019

Task 10: Single Pass Beam with Energy Recovery to October 2019

Task 11: Four Pass Beam with Energy Recovery (Low Current) December 2019

”In order to progress to Task 7, the Contractor must demonstrate to New York State Energy Research Development Authority (NYSERDA) success, in NYSERDA’s sole discretion, in meeting the goals and deliverables listed in Tasks 5 and 6. The Contractor shall not proceed with Task 7 work until it has received written approval from NYSERDA’s Project Manager to do so.”

The electron beam was transferred from 6 MeV injector, accelerated by the 36 MeV MLC and transported through the first splitter line S_1 and brought to the end of the FFA fixed field alternating gradient FFA girder made of four FFA-cells. For easier matching of the splitters with the FFA arcs single magnets half of the defocusing magnets at the beginning of the sub-section labeled FA, and at the end of the FFA arc FB is half of the focusing magnet QF were added to the regular FFA arc cells. They are of identical properties as the arc FFA magnets. The first part of this document is related to the Fractional Arc test preparation:

1. Layout
2. Instrumentation
 - a) BPM’s
 - b) Beam Arrival monitors
 - c) View-screens
3. Splitter S_1 magnets
4. Survey results in the FAT experiment
5. First prototype Fixed Field Alternating gradient girder

6. Pre-commissioning of the systems
7. Vacuum system of the S1 splitter line and of the FFA girder
8. FAT-EXPERIMENTAL RESULT. The physics results from commissioning of the CBETA Fractional Arc Test shown below are presented in two separate documents.

I. INTRODUCTION

II. EXPERIMENTAL SETUP

Layout and Description

Modeling

III. MEASUREMENTS

A. Injector Tune-up and Characterization

B. Main Linac Commissioning

RF measurement

MLC Cavity Energy Gain Calibration and Phasing

MLC Vertical offset

C. Splitter line commissioning

Beam based Magnet Calibration

Splitter Line BPM Nonlinearity Correction

Path Length Adjustment

D. Measurements at 42 MeV

Dispersion and M56

Orbit Response

Grid Scan in the Fractional FFA Arc

E. Measurements over a Broad Energy Range

Dispersion and R56

Tunes

9. Major concerns from the FAT

- MLC vertical alignment
- values of the integral magnetic field in the splitter line
- horizontal beam jitter
- survey results
- betatron and dispersion matching
- Possible MLC vacuum leak

10. Magnetic Measurements Results: FAA and splitter magnets

11. Magnet delivery and CBETA installation plan
12. CBETA vacuum system
13. DRY-RUN plans - Virtual CBETA Machine results with errors
14. Control System Training
15. Software Routines-Scripts developments
16. FFA Correction magnet system
17. Loss Monitor System
18. Beam Position Monitors and time arrival monitors of the multi energy beams
19. Safety System and Review
20. CBETA Beam commissioning plan
21. Details of remaining installation and preparation for commissioning

0.1 Layout

The whole CBETA layout is shown in Fig. 0.1.1. The Fractional arc test started with the 6 MeV electron beam from injector module 'IN', continued through the Merger, Main linac cry-module 'LA', the splitter A 'SX' and the first FFA girder. The beam will continue in March 2019 through FFA arc 'FA', transition from arc-to-straight 'TA', the straight section made of three modules 'ZA', 'ZM', and 'ZB', continues with the second transition from the straight-arc FFA 'FB' and finishes through the second Splitter B and merger to the MLC. The S1 splitter beam line final installation photograph with the fixed field magnet girder is shown in Fig. 0.1.2.

0.2 Instrumentation - BPM's, Beam Arrival Monitors, Beam Profile Monitors

There are 160 Beam Position Monitor modules (BPM's) using the BNL designed V301 VME-based hardware. The BPM analog to digital converters (ADC) are timed to peak of the selected energy bunch and will compute position based on the raw data sample. Many measurements are averaged. The BPM's will measure one energy beam at the time and will sequence through the different energies by changing the beam trigger timing. There will be sixteen Beam Arrival Monitor (BAM) modules using V301 module and CU designed RF mixer chassis to be used for energy measurements in each of the 8 splitter lines. The BAMs used two dedicated BPM buttons in the S1 splitter line the first and last one. The BPM hardware configuration for acquiring button BPM data with single sample at peak of each bunch, shown in Fig. 0.2.1, is using the BNL V301 boards as a base. The 50 MHz beam synchronous RF clock is distributed to V301 module via VME backplane through the V208 module. The 50 MHz RF clock is

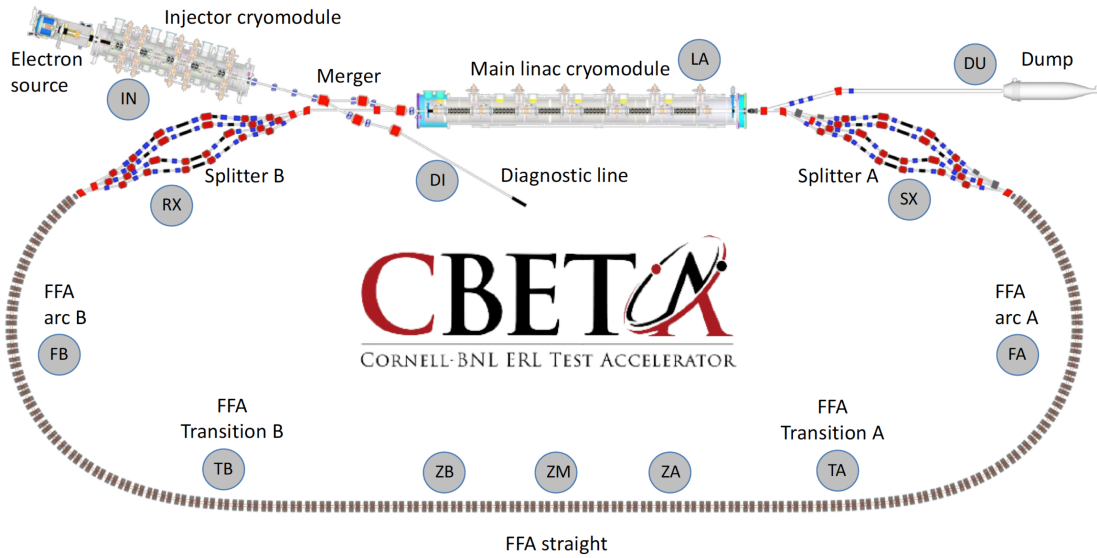


Figure 0.1.1: The CBETA machine layout.



Figure 0.1.2: The final step in installation of the Fractional Arc Test (FAT).

multiplied up to 400 MHz in a PLL within the V301 module. The ADC data are required using the 400 MHz clock that is locked to the 50 MHz clock. A beam trigger signal from the RF system is used to initiate acquisition of the raw ADC data. Details of the hardware

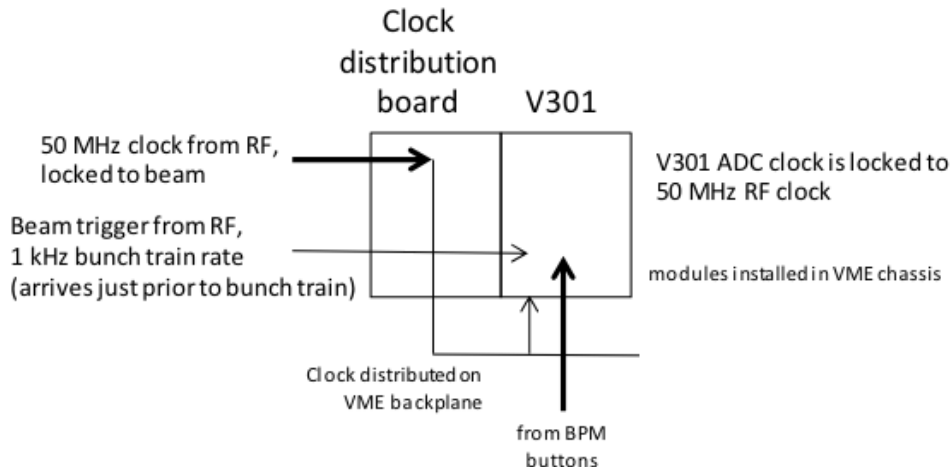


Figure 0.2.1: Fractional Arc Test: Technique for measuring beam positions at the peak of each bunch setup are shown in Fig. 0.2.2. For the Fractional Arc Test fifteen V301-BNL modules have

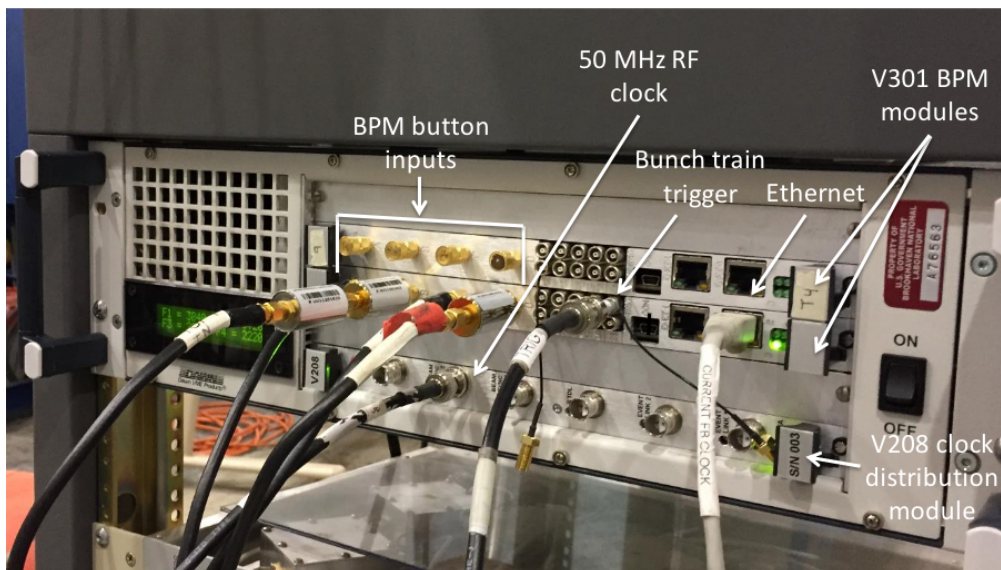


Figure 0.2.2: Fractional Arc Test: Technique for measuring beam positions at the peak of each bunch

been modified with the Bessel filter and inductor change. There are two configurations: one pass and four-pass machine and 160 modules V301 are being delivered and are in the process of PC board acceptance. The real FAT BPM data are shown in Fig. 0.2.3 The beam profile monitors or view-screens design in shown in Fig. 0.2.4. More details about the BPM system is provided in a separate document by Robert Michnoff. The view-screens placed in the S1

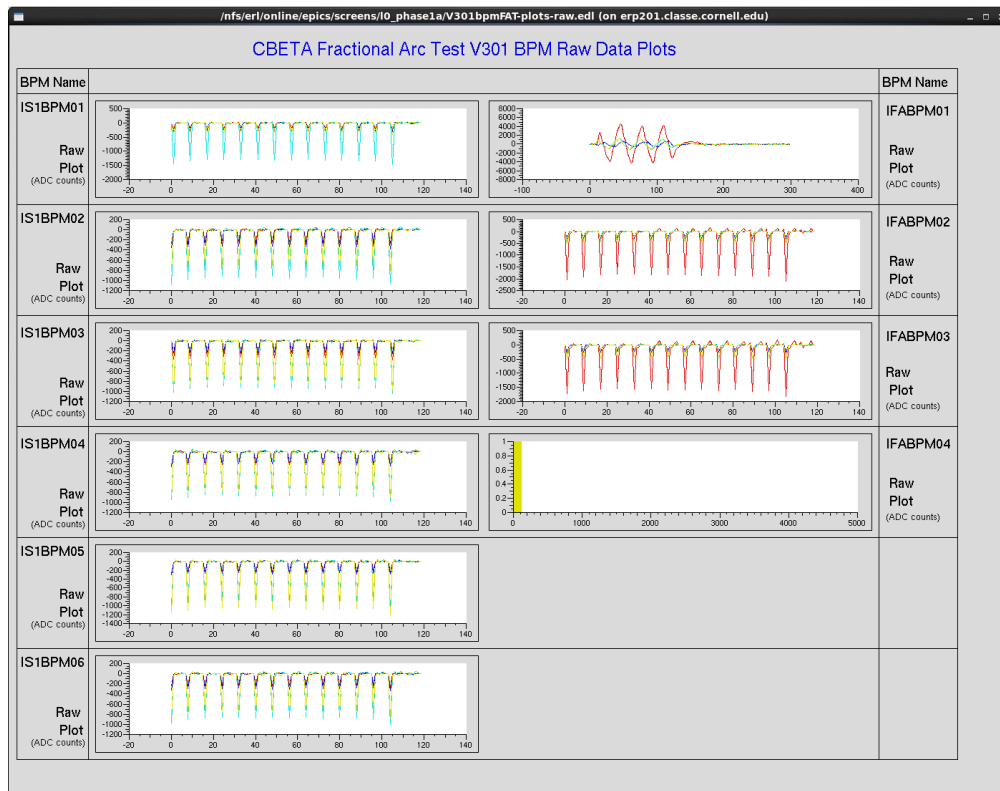


Figure 0.2.3: CBETA Fractional Arc Test V301 BPM Raw Data Plots.

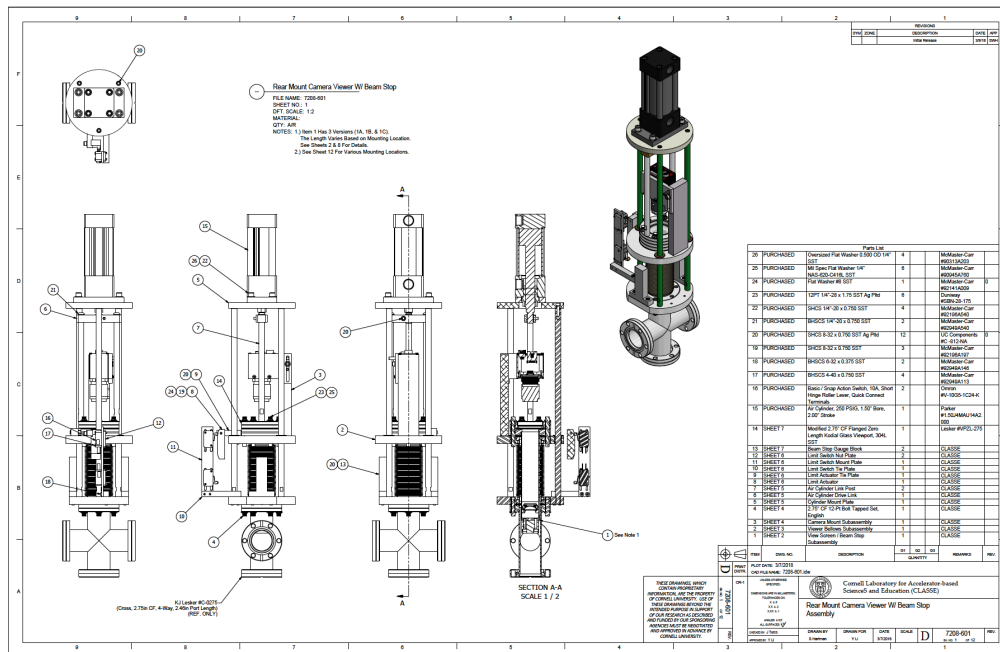


Figure 0.2.4: Beamprofile monitor design.

splitter line are shown in Fig. 0.2.5. Details of the view-screens in the first FFA girder are

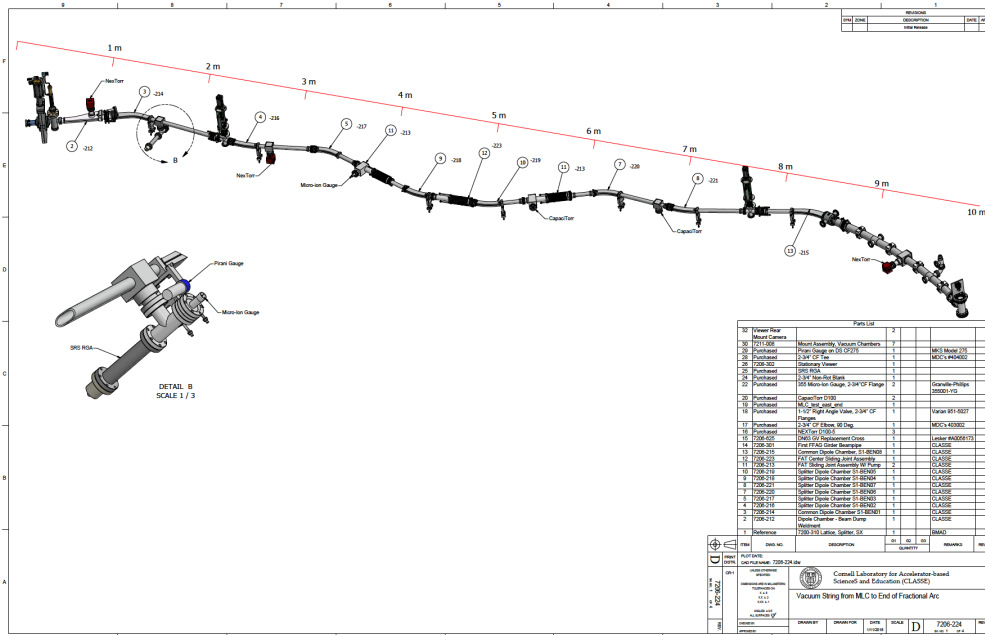


Figure 0.2.5: Vacuum system of the splitter line with the view-screens.

shown in Fig. 0.2.6. The beam profile from the first view screen of the S1 splitter line is shown in Fig. 0.2.7. It is important to note that the first beam profile monitor-view screen is located downstream of the common dipole. Electrons with the higher momentum will be bend less and will show on the left side of screen. During the phase adjustments of the MLC cavities the shape of the beam viewed on this screen can be used to determine if the bunch is located longitudinally at the top of the RF sinusoidal function as the beam profile after the bend will be symmetric.

0.3 Splitter S1 magnets

Different types of the Splitter magnets are shown in Fig. 0.3.1. The S1 splitter beam line used in the Fractional Arc Test is shown in Fig. 0.3.2. A connection of the splitter line to the MLC one side and to the FFA on the other side are shown in Fig. 0.3.3 and Fig. 0.3.4, respectively. The S1 splitter line 42 MeV electron beam time of flight is designed and built to provide half of the required time adjustment for the first turn energy recovery mode. The chicane elements will be repositioned for the multi energy recovery mode. But for the fine adjustment of the time of flight in the S1 splitter line a special sliding joints with longer bellows are designed, installed (as shown in Fig. 0.3.5) and tested during the Fractional Arc Test, as shown in Fig. 0.3.6. Three positions of the sliding joints are shown in Fig. 0.3.7

Installation of the magnets before the Fractional Arc test are shown in few photographs Fig. 0.3.8 and Fig. 0.3.9.

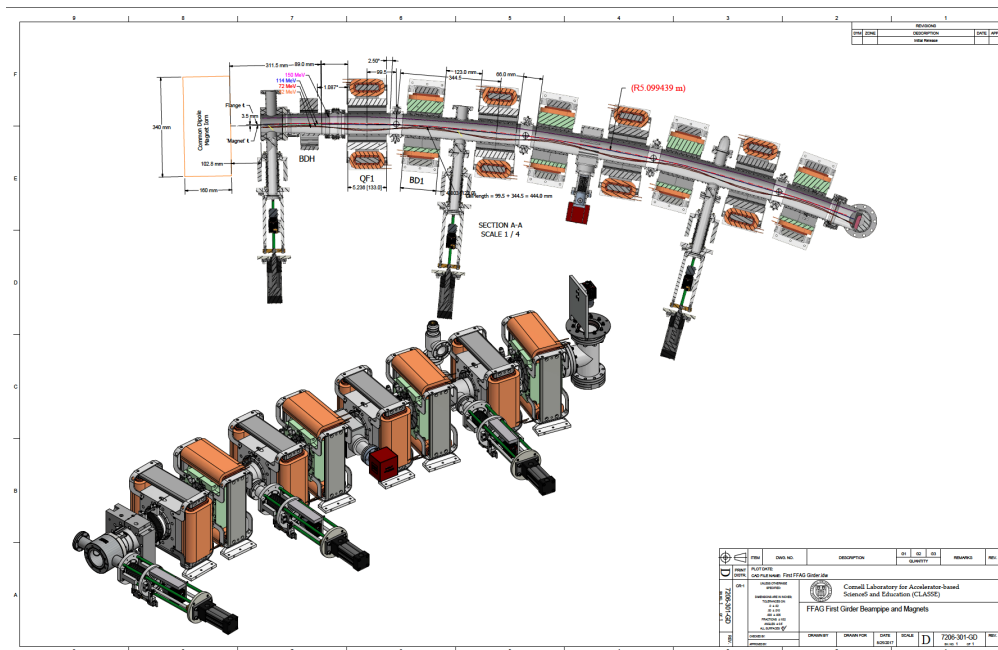


Figure 0.2.6: Viewscreens in the FFA first girder for the fractional arc test.

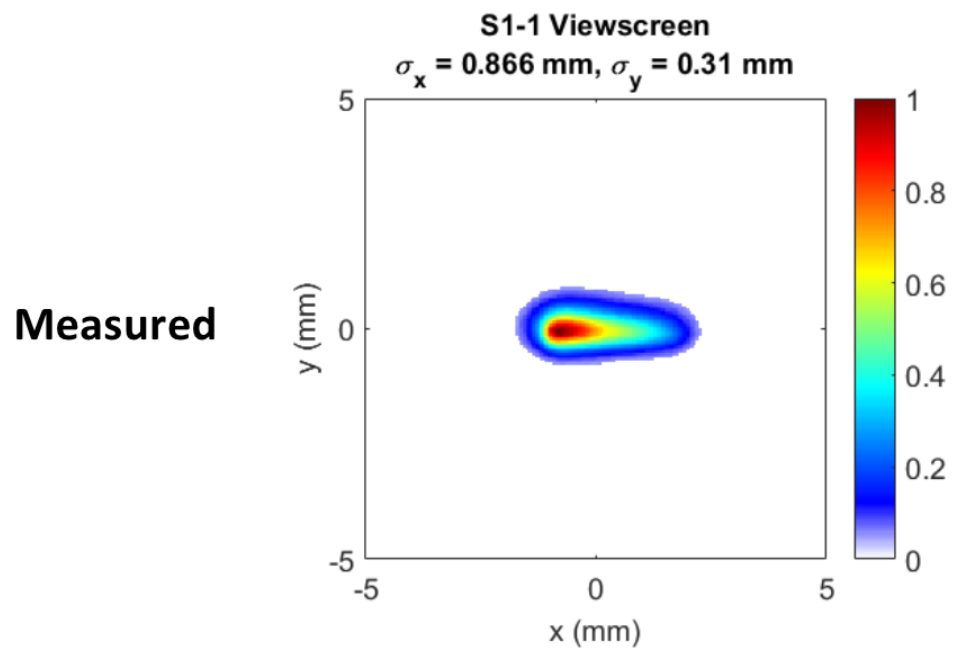


Figure 0.2.7: Beam profile result shown in the first view-screen.

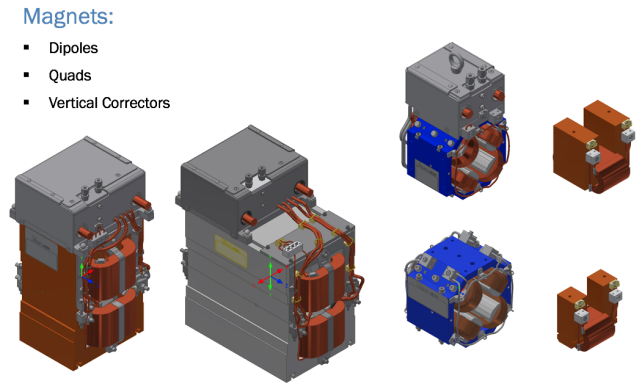


Figure 0.3.1: Types of the magnets in S1 splitter line.

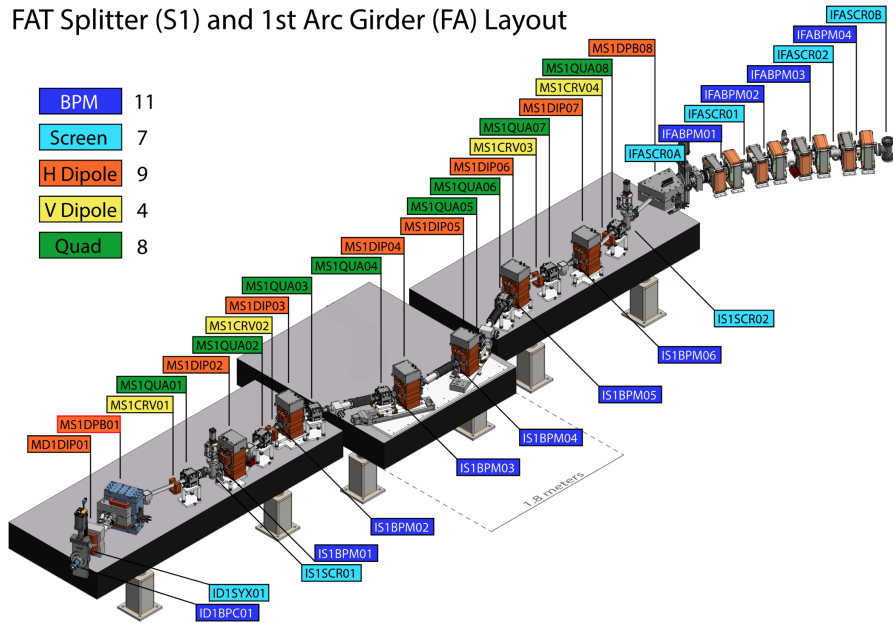


Figure 0.3.2: The splitter line S1 together with the first FFA girder.

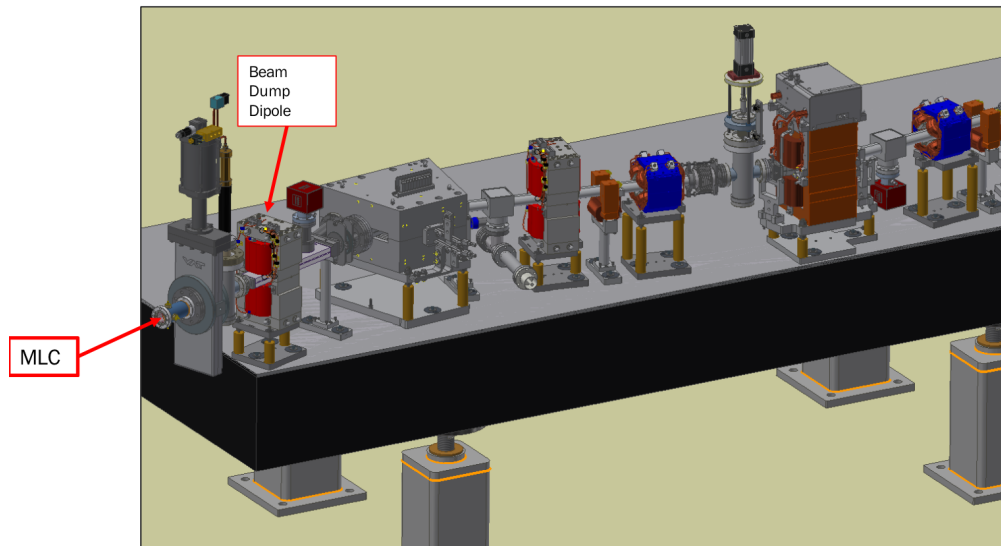


Figure 0.3.3: Connection of the S1 splitter line to the MLC.

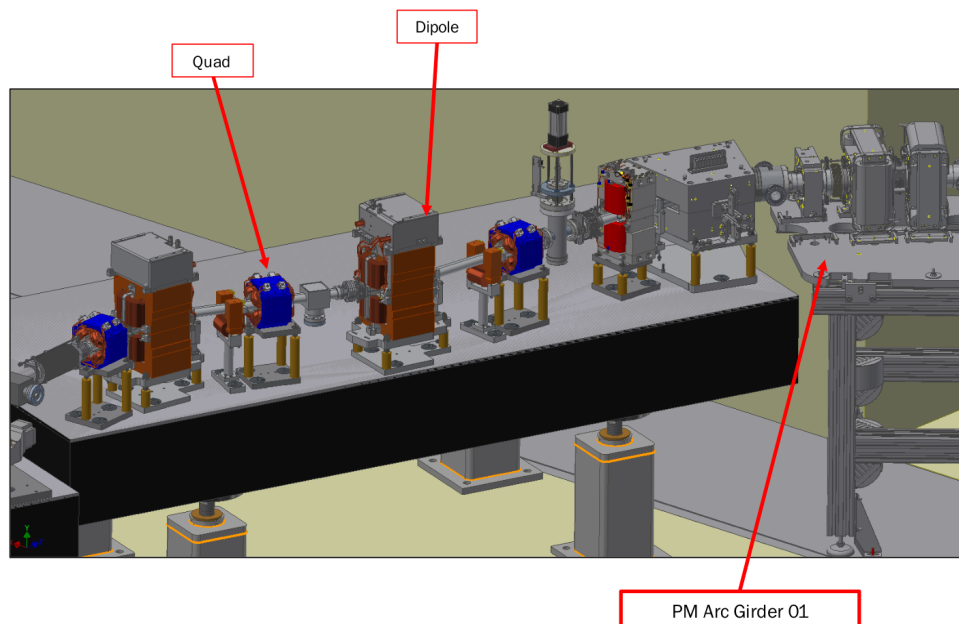


Figure 0.3.4: Connection of the S1 splitter line to the FFA first girder.

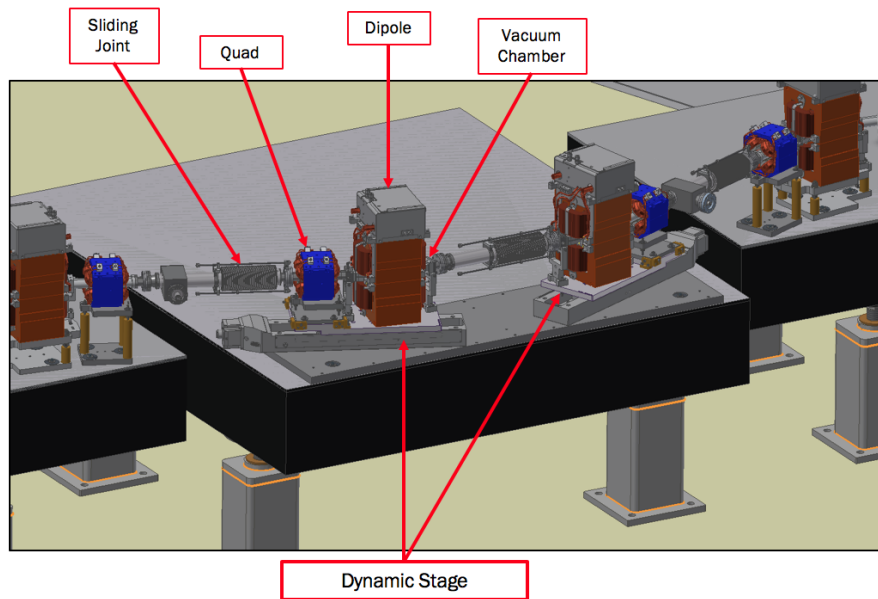
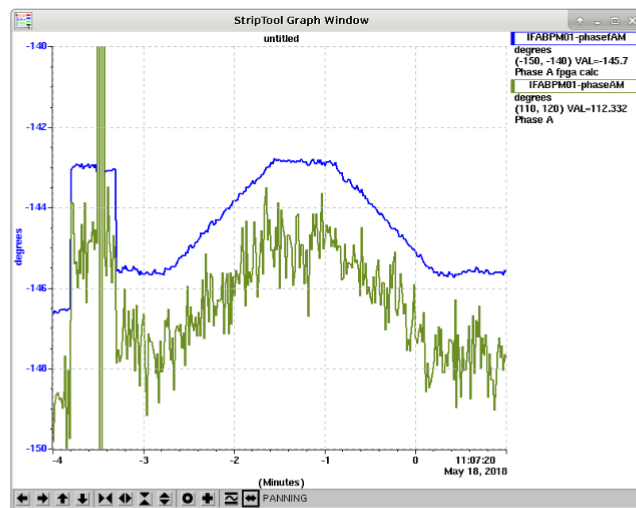


Figure 0.3.5: The splitter line S1 fine time of flight adjustment.



Command 1 cm travel: Stage moved 2.8 degrees on S1 BPM #6 (temporarily wired as a BAM)

- 2.8 degrees = **1.8 mm** of path length change
- $2 \times (1 - \cos \theta) \times (1 \text{ cm}) = \mathbf{1.63 \text{ mm}}$ for $\theta = 23.3$ degrees

Figure 0.3.6: Measurement results of the position and electrons time of flight.

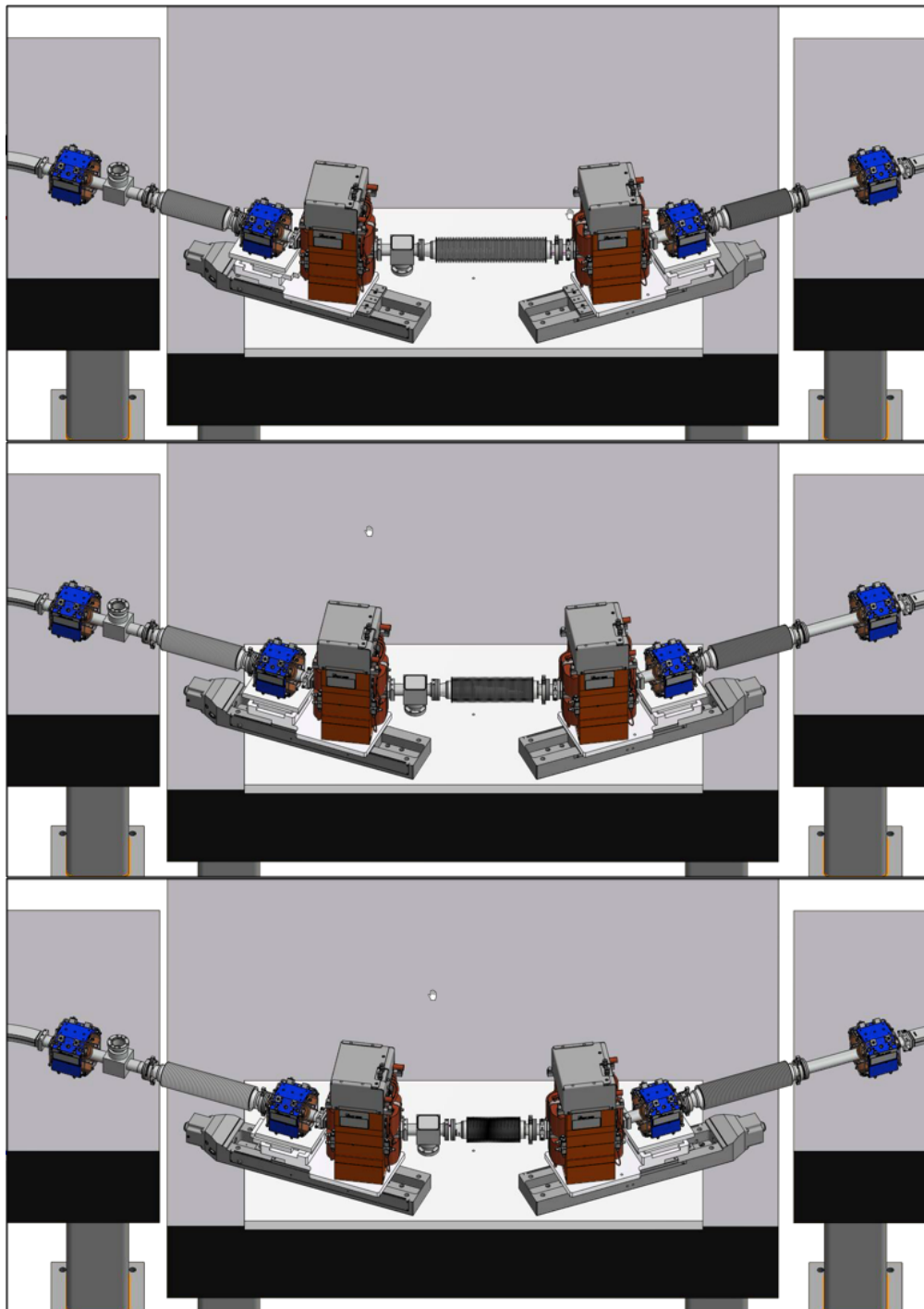


Figure 0.3.7: Three positions of the S1 splitter line sliding joints for the fine timing adjustment.

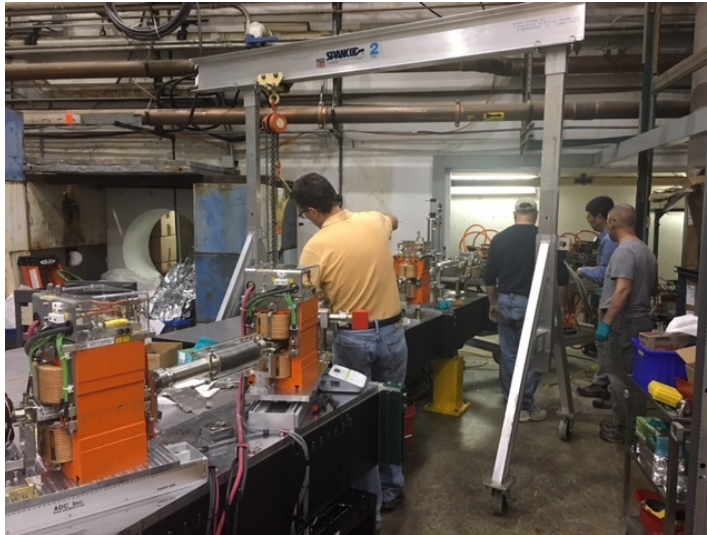


Figure 0.3.8: Installation of the splitter magnets on the three supporting tables.

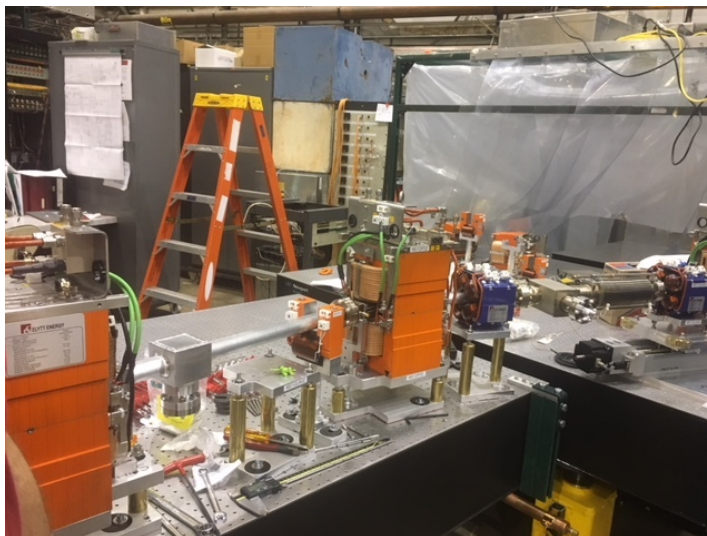


Figure 0.3.9: Installation of the splitter magnets on the three supporting tables.

0.4 Survey results in the Fractional Arc Test

There were two survey runs of the FFA prototype girder. The first results are shown in Fig. 0.4.1, while the second correction survey results are shown in Fig. 0.4.2.

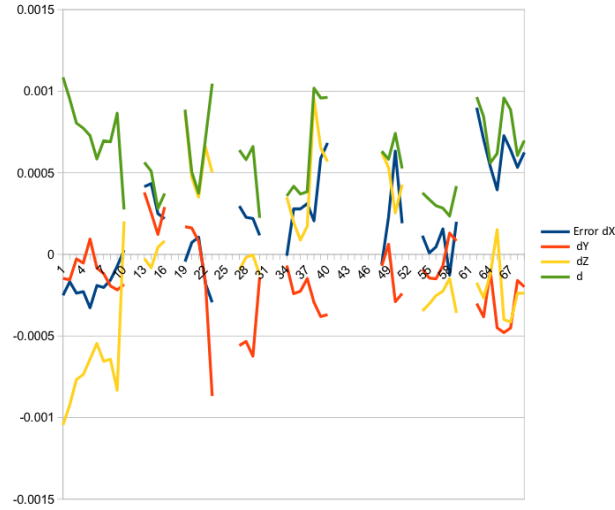


Figure 0.4.1: Results from the survey of the FFA magnets on the prototype girder during the FAT test. Units of the vertical axis are in meters. Error in the survey is shown by the blue lines.

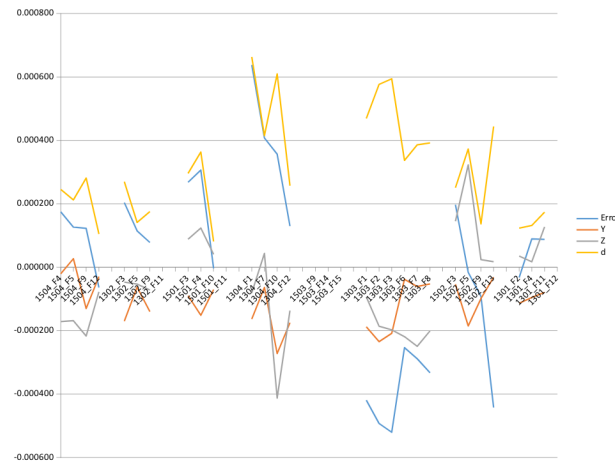


Figure 0.4.2: Results from the second correction run survey of the FFA magnets. Units of the vertical axis are in meters. Total errors in the survey is shown by the blue lines.

0.5 First Prototype Fixed Field Alternating gradient girder

The first prototype girder has four base FFA cells with a half defocusing magnet in from of them to allow easier matching of the betatron and dispersion function to the splitter line S1. A design of the last FFA girder is shown in Fig. 0.5.1.

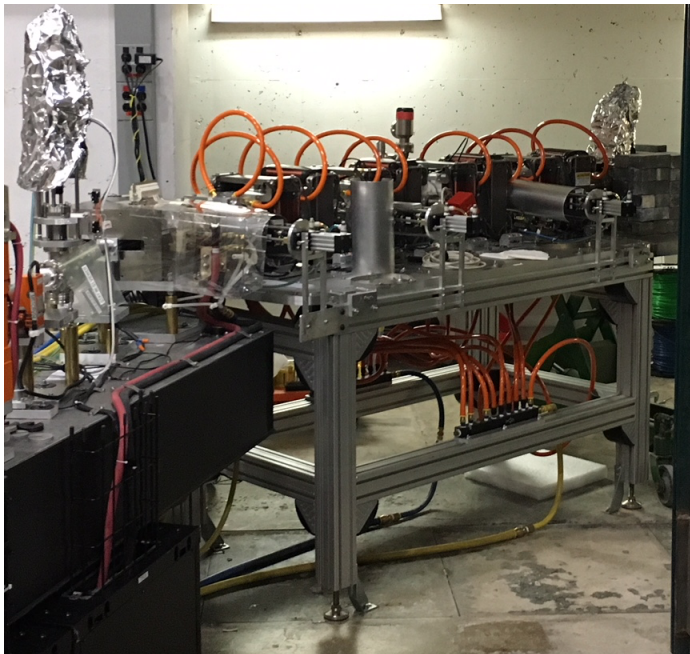


Figure 0.5.1: The photograph of the last part of the FAT beam line test shows the FFA girder and connection to the S1 beam line.

The final stage in production of the first prototype girder is shown in the photograph Fig. ??

0.6 Pre-commissioning of the systems

The S1 magnet polarities were tested by using the Hall probe. Couple of errors in the magnets cable connections were found and corrected. New instructions were sent to the magnet production company Elyte to prevent future errors. The dipole magnets were tested with the beam as shown in Fig. 0.6.1 and at different energies Fig. 0.6.2.

0.7 Vacuum system of the splitter line and of the FFA single beam line

The vacuum system development for the Fractional Arc test is shown in Fig. 0.7.1.



Figure 0.5.2: The photograph of the last stage in production and assembly of the first fixed field magnet girder.

Table 0.7.1: Magnet component count for S1 splitter line.

section	Dipole	Septum	Quad	BPM	Corrector (V)
S1	8	0	8	8	4

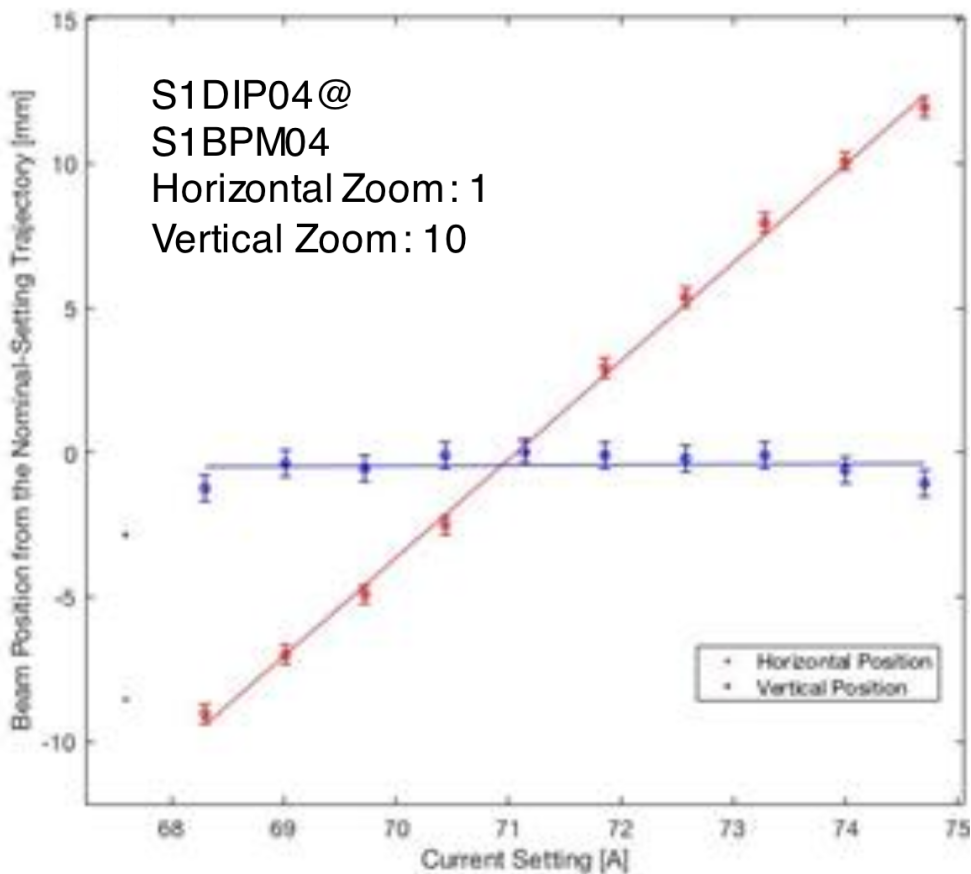


Figure 0.6.1: Vertical and Horizontal positions dependence on the dipole excitation currents

File:	Bend angle (horizontal) at Nominal Current [Radians] $\frac{\Delta\theta}{\Delta I} \cdot I_{nom}$	Bend angle (vertical) at Nominal Current [Radians]	Horizontal Bend Angle / Current [Radians/Amp] $\frac{\Delta x}{\Delta I} \cdot \frac{1}{M_{12}} = \frac{\Delta\theta}{\Delta I}$	Vertical Bend Angle / Current [Radians/Amp]	Calibration Value [Tesla Meters/Amp] $\int \alpha \cdot dl = \frac{\Delta\theta}{\Delta I} \cdot \frac{p}{e}$	Expected Field Integral Along Trajectory [Tesla Meters/Amp]	Roll Angle [Radians] $\frac{\Delta y}{\Delta x} \cdot \frac{\pi}{2}$
42MeV Quads Off	NA	NA	NA	NA	NA	6.98e-04	NA
Full Corrector Range 42MeV	4.12e-01 ± 1.1e-02	5.6e-04 ± 9.1e-04	5.29e-03 ± 1.4e-04	7.e-06 ± 1.2e-05	7.40e-04 ± 1.9e-05	6.98e-04	2.1e-03 ± 3.5e-03
38MeV Scan	4.495e-01 ± 6.9e-03	2.1e-04 ± 9.3e-04	6.318e-03 ± 9.7e-05	3.e-06 ± 1.3e-05	8.00e-04 ± 1.2e-05	6.98e-04	7.e-04 ± 3.3e-03
47MeV Scan	4.449e-01 ± 5.7e-03	-8e-05 ± 1.9e-03	5.067e-03 ± 6.5e-05	-9e-07 ± 2.2e-05	7.94e-04 ± 1.0e-05	6.98e-04	-3.e-04 ± 6.7e-03
53MeV Scan	4.436e-01 ± 3.5e-03	-1.e-04 ± 1.6e-03	4.451e-03 ± 3.5e-05	-1.e-06 ± 1.6e-05	7.863e-04 ± 6.2e-06	6.98e-04	-4.e-04 ± 5.7e-03

Figure 0.6.2: Bending angle dependence on the currents in the dipoles for different energies - transfer function calibration



Figure 0.7.1: Vacuum system development for the S1 splitter line.

0.8 Magnetic Measurements Results: FAA and splitter magnets

The ELYTT company from Spain is providing magnetic field measurement scanned in the horizontal plane. In addition there is a plan to do the detail Hall probe measurements at NSLS-II measurement facility of the couple of S1 magnets. The measurement results from ELYTT are being transferred to the CBETA team.

0.9 Magnet delivery and CBETA installation plan

The magnet production for the fixed field FFA arcs and straight sections is progressing according to the plan with the last magnet to be produced at the end October 2018 and shipped immediately by air. There are five different types of magnets being produced by KYMA company as shown in Fig. 0.9.1. Locations of specific fixed field magnet types in the FFA arcs and straight section is shown in Fig. 0.9.2. The production and testing flow presented by Stephen Brooks is shown in the diagram below Fig. 0.9.3. The permanent magnet wedge blocks designed by BLN are ordered and made in China from the company "AllStar" located in Vancouver, Canada. Full strength and orientation tests of the magnet blocks are provided by the producer but not with the temperature control, while the partial (15%) test-verification of the blocks strength and orientation was tested at BNL with the Helmholtz coil measurements (the coil was built by 'KYMA', a company located in Italy and Slovenia). The Helmholtz measurements results of the magnetization angle distribution (Stephen Brooks) are shown in Fig. 0.9.4. The results of the magnet field simulation with errors of the magnetic field strength, field angle and positions by Stephen Brooks are shown in Fig. 0.9.5. From the previous experience in building the prototype girder, it became clear that replacement of the P15 and P16 magnetic blocks would be preferable. The remainder of wedge blocks was shipped directly from China to KYMA company and were tested in KYMA with their own Helmholtz coil.



Figure 0.9.1: CBETA fixed field type of magnets and their parameters.

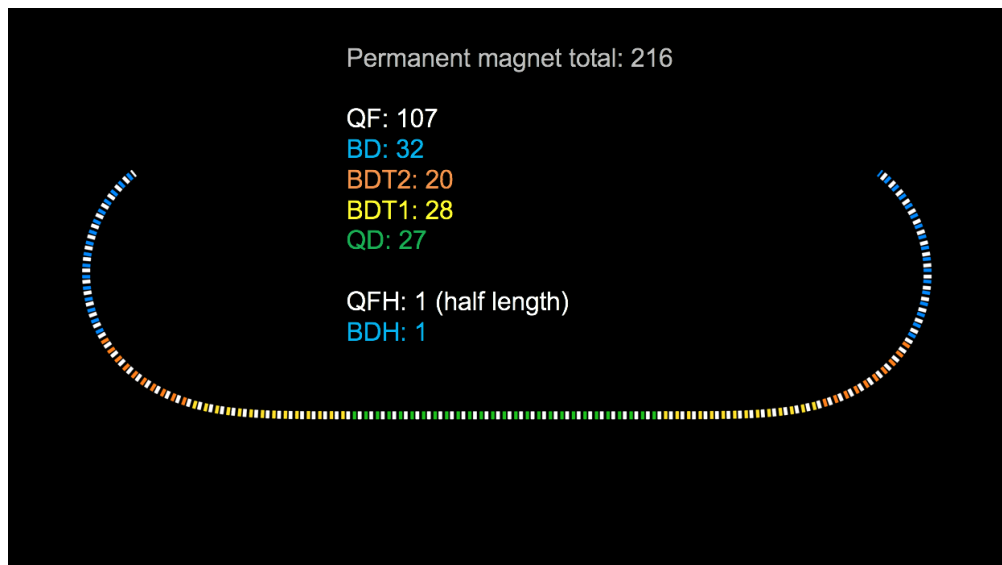


Figure 0.9.2: Fixed Field magnet distribution in CBETA permanent magnet sections.

The magnets were assembled (as shown in Fig. 0.9.6 in KYMA in Slovenia and shipped in the boxes (as shown in Fig. 0.9.7) by air to BNL. In BNL there are couple of rotating coil measurements: one before corrections, including the survey of the magnet fiducials with a harmonic coil alignment to the center of the magnet, and the second to sometimes third harmonic coil measurements after the harmonic wire corrections. The harmonic coil measurement is shown in Fig. 0.9.9.

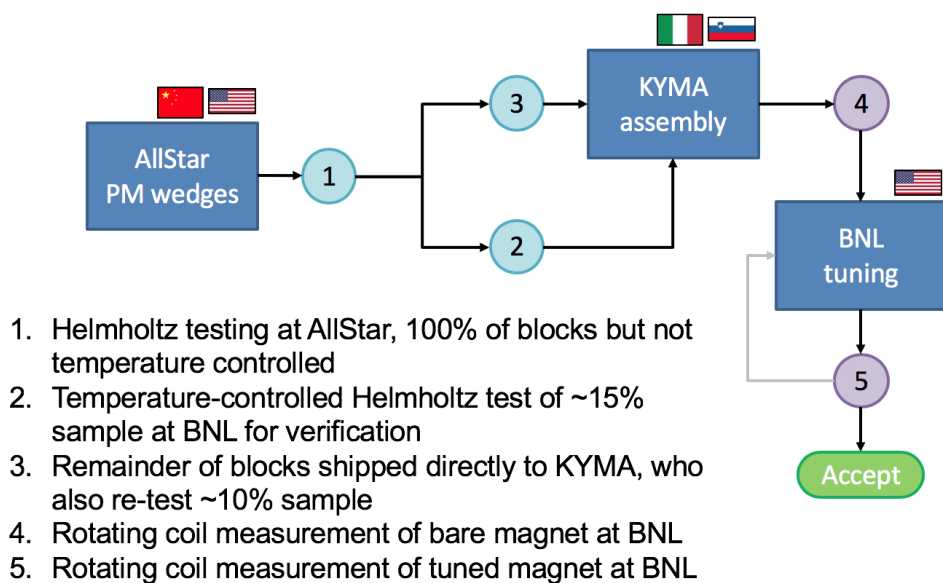


Figure 0.9.3: Production and testing flow of the FFA magnets in CBETA.

The magnet production rate by the type of magnets is shown in Fig. ??, while the tuning rate, the final step in the magnet production, is shown in Fig. 0.9.8, respectively.

The projection for the last magnet delivery from the existing data are shown in Table 0.9.1.

Table 0.9.1: Magnet component count for S1 splitter line.

Method	Rotating Coil Measurements	Magnets Tuned per week	Projected Finish date	Speed-up requirement
Magnets rate since main production started		9.92	Nov 26	4 calendar days spare
Rotating coil rate since start	26.9	10.76	Nov 20	10 calendar days spare

The magnet quality criteria are shown in Table 0.9.2. The square root of the sum of all multipole units squared defined as $FOM = \sqrt{\sum (multipoles)^2}$. Results of the magnetic strength and values of the magnetic field multipole errors are shown in Fig. 0.9.10 and Fig. 0.9.11. Results from the tuned integral field errors are shown in Fig. 0.9.12.

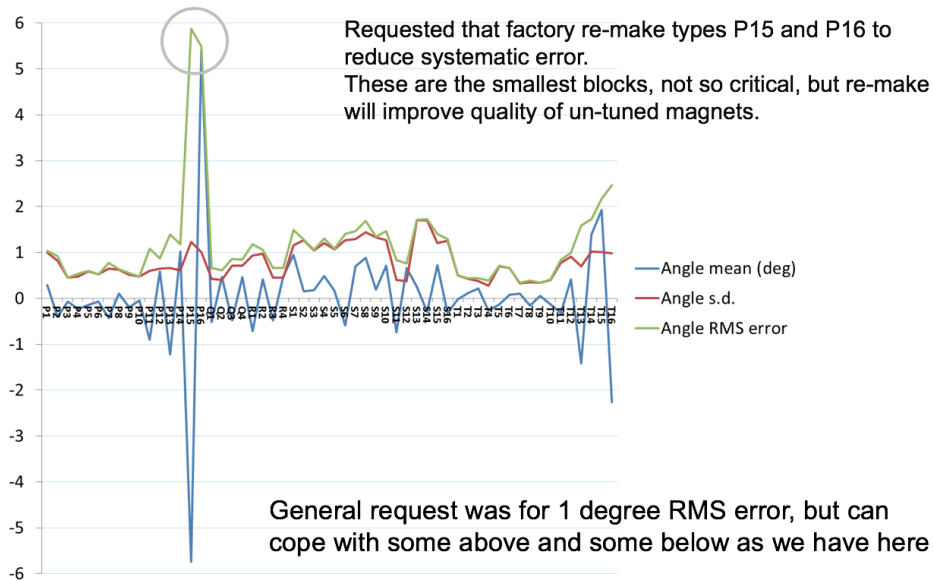


Figure 0.9.4: Permanent magnet blocks magnetization error. Two permanent magnet blocks (P15 and P16) had to be reordered as the magnetization error was too large.

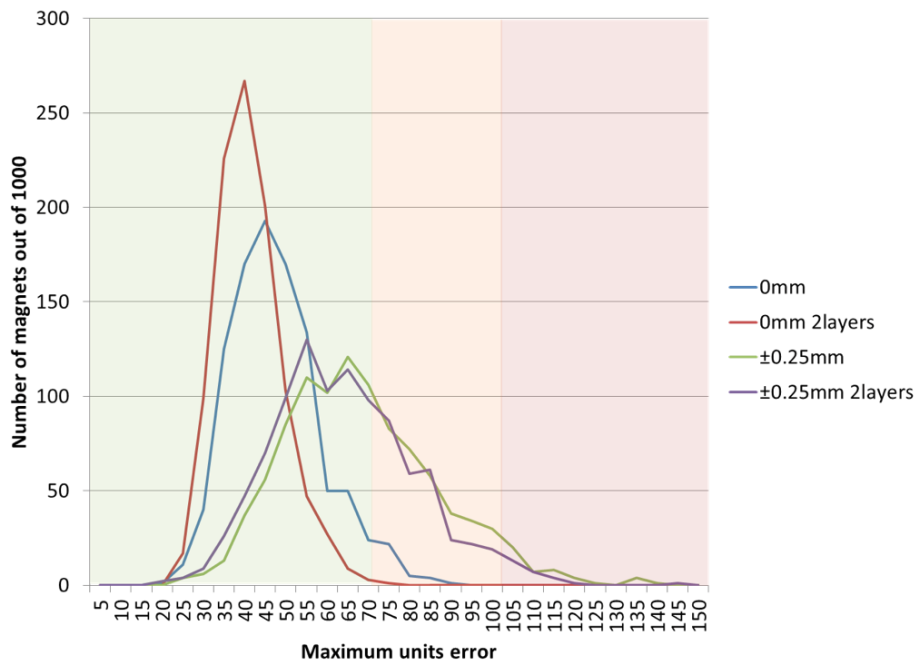


Figure 0.9.5: 1000 magnets were generated some with position errors. Histogram is binned by unit FOM. The green color shows that these magnets are easy to tune, from the previous experience in building the prototype girder, red color indicates possible problems in tuning the magnets - Stephen Brooks.

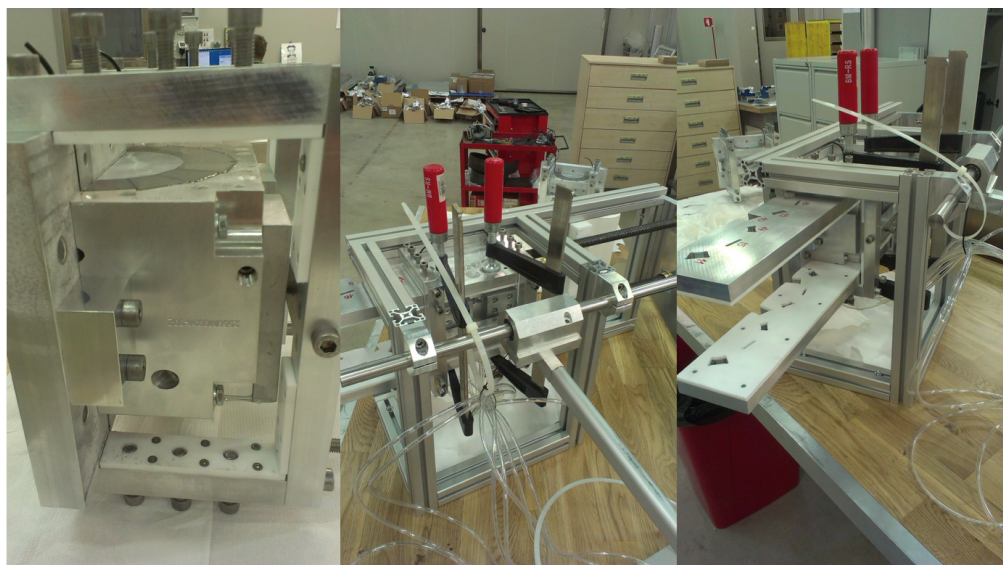


Figure 0.9.6: Special assembly structures for the permanent magnet installation.



Figure 0.9.7: Due to a very strong magnetic field the assembled magnets needed to be safely packed in the boxes, separate from each other, for air transport.

Table 0.9.2: Tuned Magnet Criteria.

Mid-plane error (G)	Units FOM	CBETA FOM	Quad error at x=0 (res.)
≤ 1.5	≤ 10	≤ 0.375	$\leq 0.05\%$

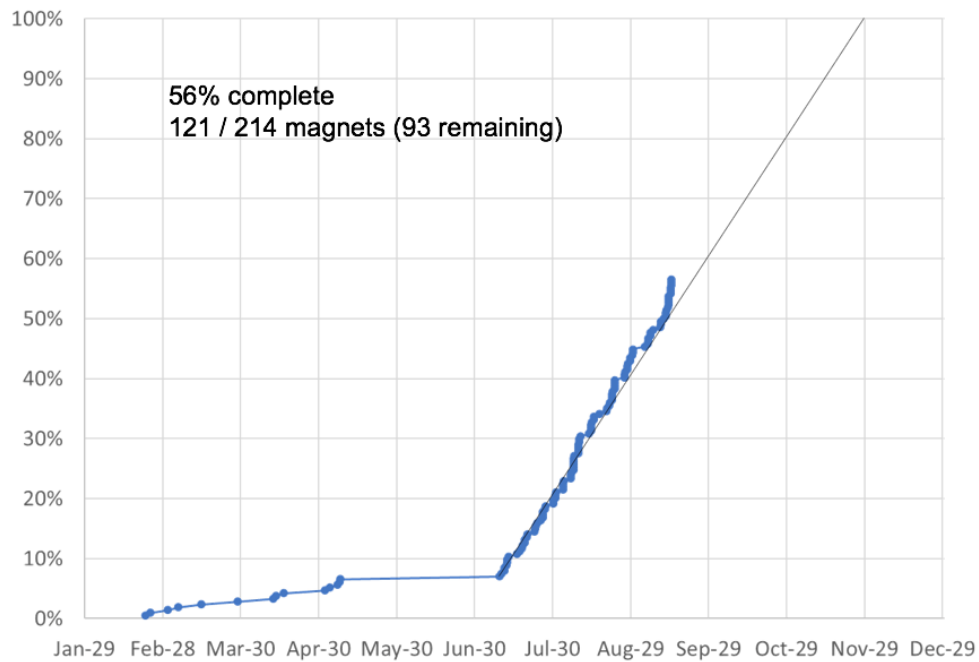


Figure 0.9.8: Predictions of the final magnet production - magnet measurements after tuning.

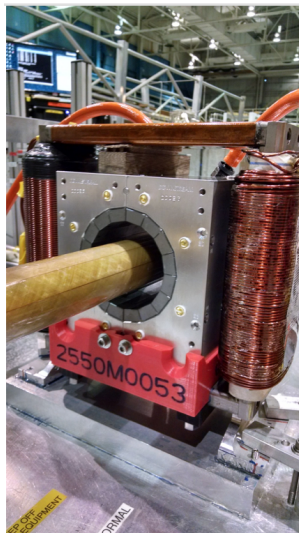


Figure 0.9.9: Harmonic coil measurement with the KYMA magnet and iron correction magnet around it.

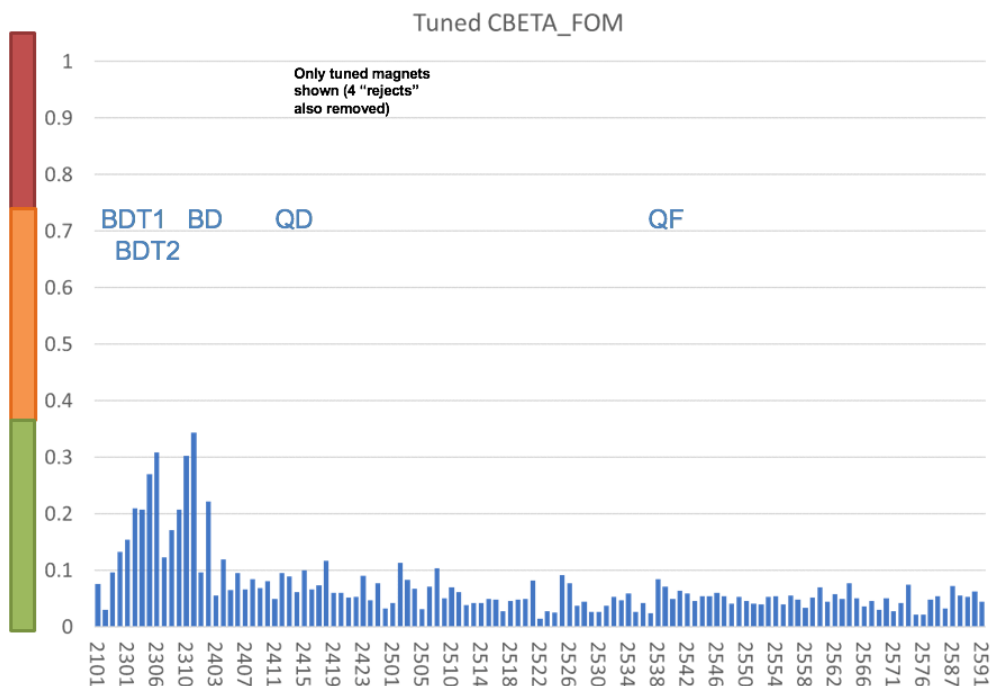


Figure 0.9.10: Results of the tuned magnets in FOM (square root of the sum of all multipoles in the magnet squared).

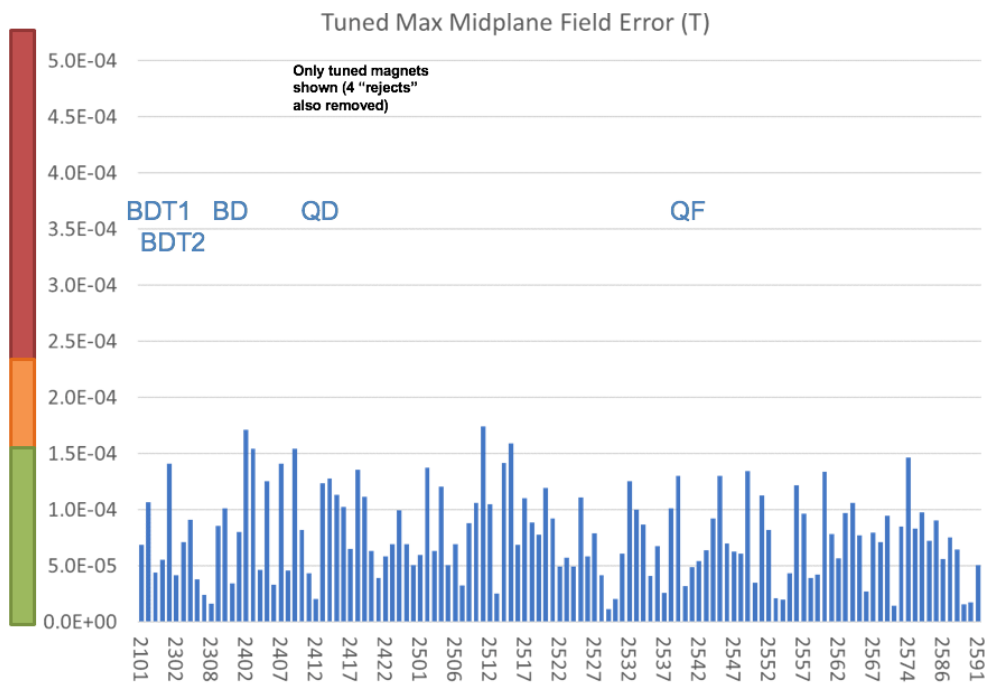


Figure 0.9.11: Results of the integral field errors after the magnets were tuned.

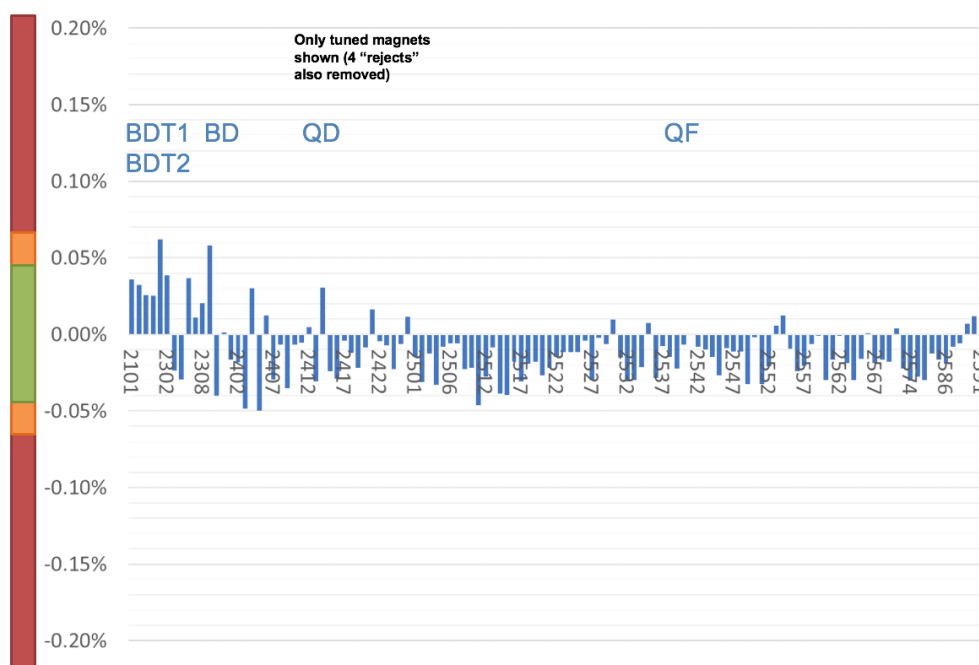


Figure 0.9.12: Integral field error after the magnets were tuned. The vertical axis units is in %

The CBETA FFA magnet girder production is in the final stage as shown in Fig. 0.9.13 and the correction harmonic iron wires placed in the plastic folders are shown in Fig. 0.9.14

0.10 CBETA vacuum system

A complete design of the CBETA vacuum system is shown in Fig. 0.10.1. Details are shown in the three parts: 1. The fixed field magnet FFA line shown in Fig. 0.10.2, 2. Four splitter beam lines with orbits from the linac MLC (S1, S2, S3, and S4) are shown in Fig. 0.10.2, and Fig. ??, respectively. Details of the vacuum pipe at the beginning of the splitter lines are shown in two figures Fig. 0.10.4 and Fig. 0.10.5. 3. The combiner beam lines return to the linac from the FFA arc (R1, R2, R3, and R4). Details of the single fixed field vacuum pipe design and one already built are shown in Fig. 0.5.1 and Fig. 0.10.6 respectively. The survey data of the FFA vacuum pipe are shown in Fig. 0.10.7. A design of the BPM, a part of the vacuum system, together with the built BPM is shown in Fig. 0.10.8. The FA arc design together with details of a single cell is shown in Fig. 0.10.9.



Figure 0.9.13: The FFA magnets are installed on the girders after the field correction is finalized.



Figure 0.9.14: The 3D printer support plastic folders for the magnetic field corrections with iron wires.

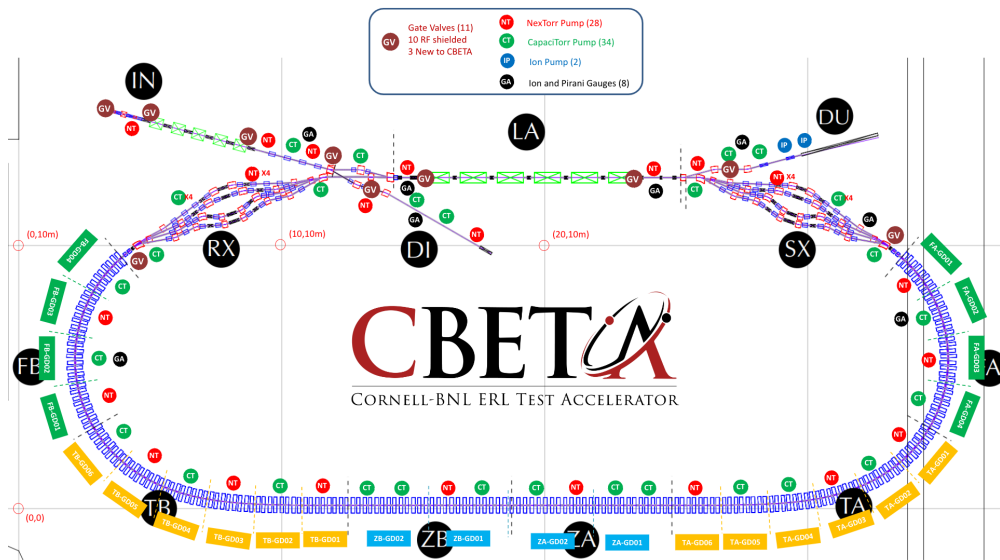


Figure 0.10.1: Vacuum system design for the return beam line with the fixed field magnets(FFA-part).

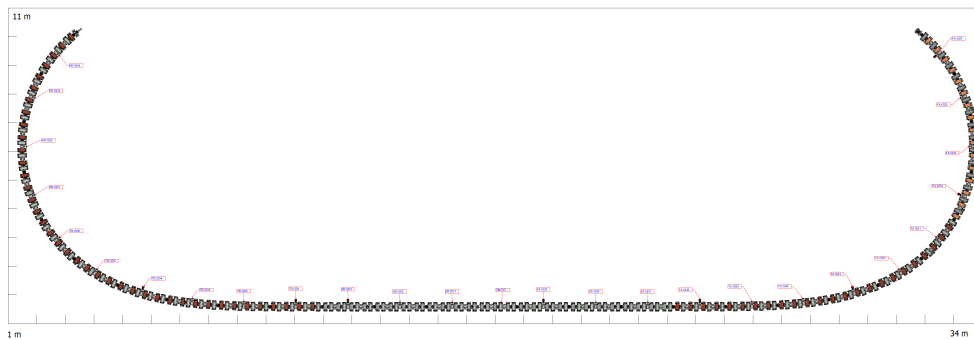


Figure 0.10.2: Vacuum system design for the return beam line with the fixed field magnets(FFA-part).

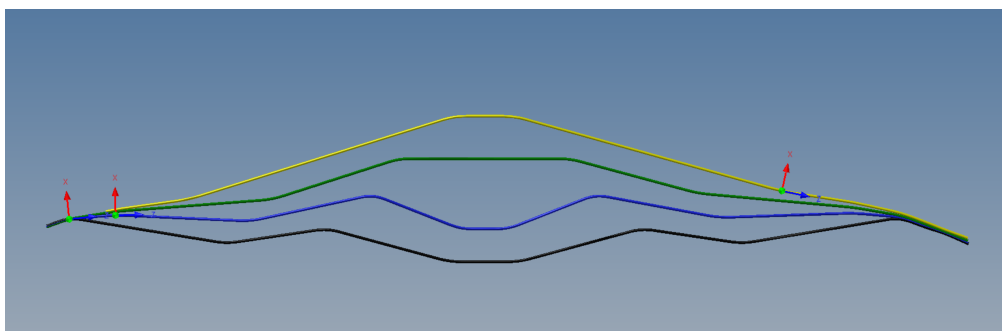


Figure 0.10.3: Four splitter beam lines

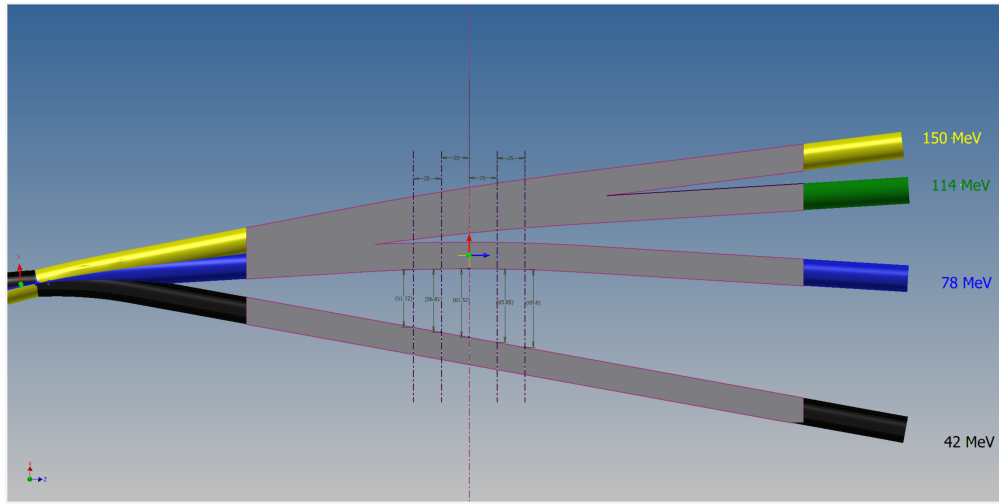


Figure 0.10.4: Details of the vacuum pipe design at the beginning of the splitter section.

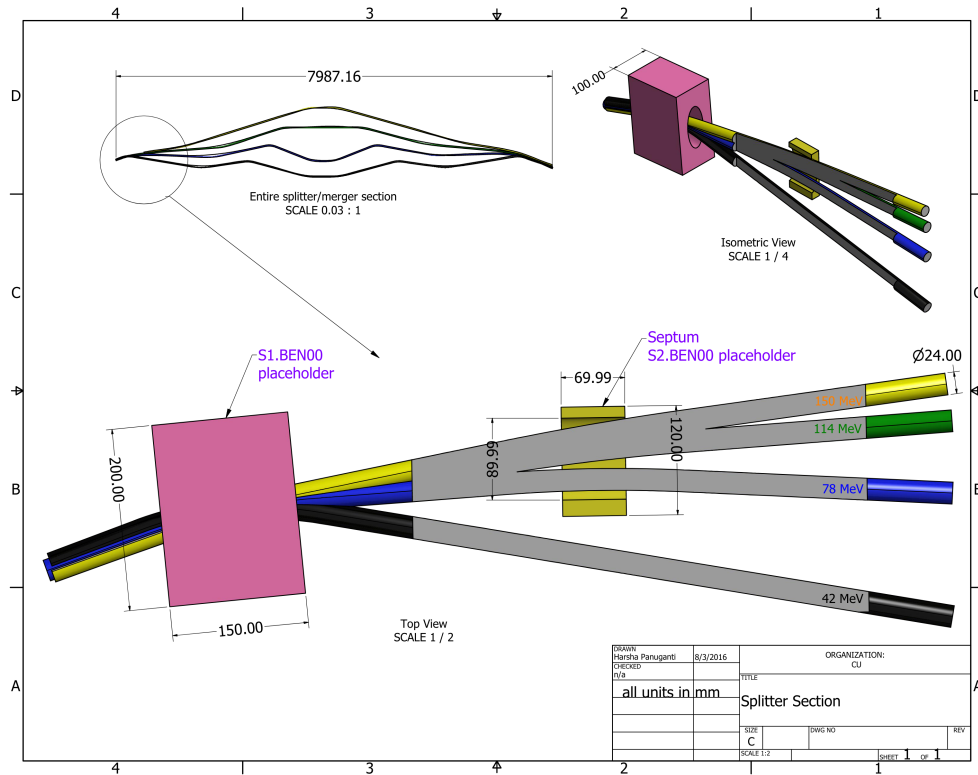


Figure 0.10.5: Beginning of the splitter section with the common dipole and first septum.

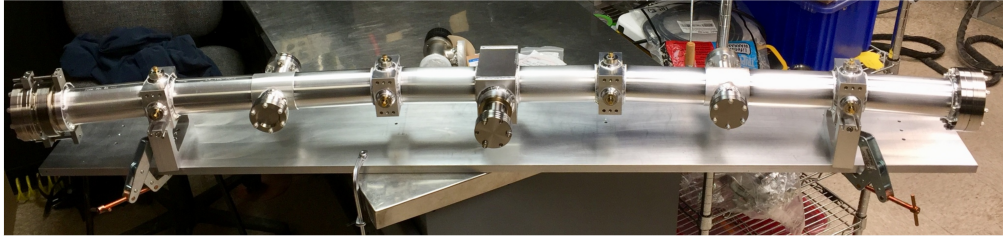


Figure 0.10.6: The single FFA arc vacuum pipe built with BPM's and vacuum connections.

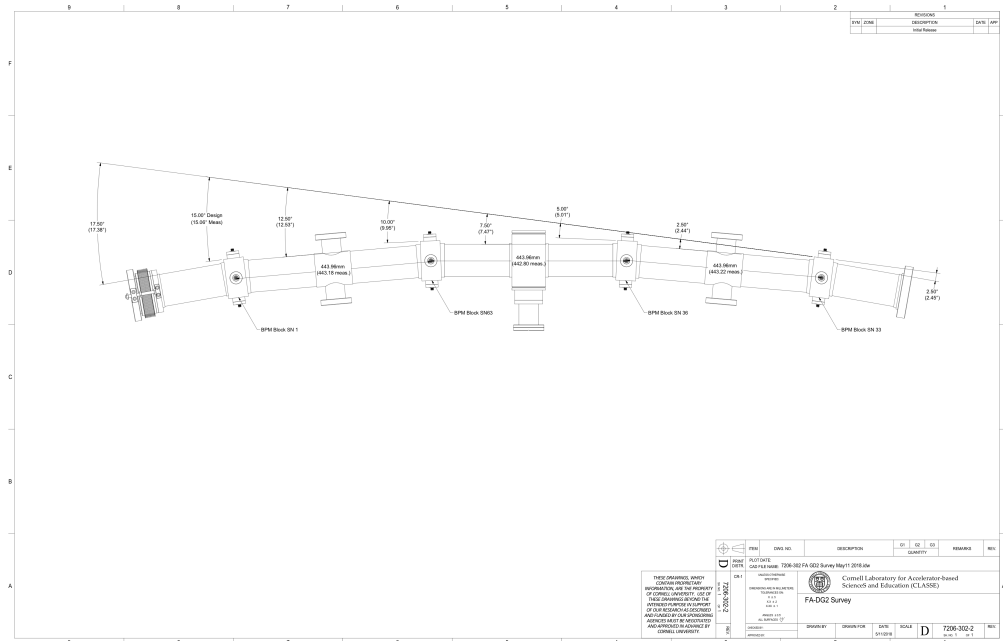


Figure 0.10.7: Details of the survey FFA vacuum pipe results.

Block Number	Coaxiality 1 Dev	Coaxiality 2 Dev	Coaxiality 3 Dev	Coaxiality 4 Dev	Comments	Assembly/Weld Date
1	0.003	0.001	0.002	0.002	Good	Welded 9/5/17
33	0.002	0.002	0.001	0.003	Good	Welded 9/5/17
36	0.002	0.002	0.002	0.003	Good	Welded 9/5/17
63	0.002	0.002	0.004	0.002	Okay	Welded 9/5/17

Figure 0.10.8: A BMP design together with a built BMP.

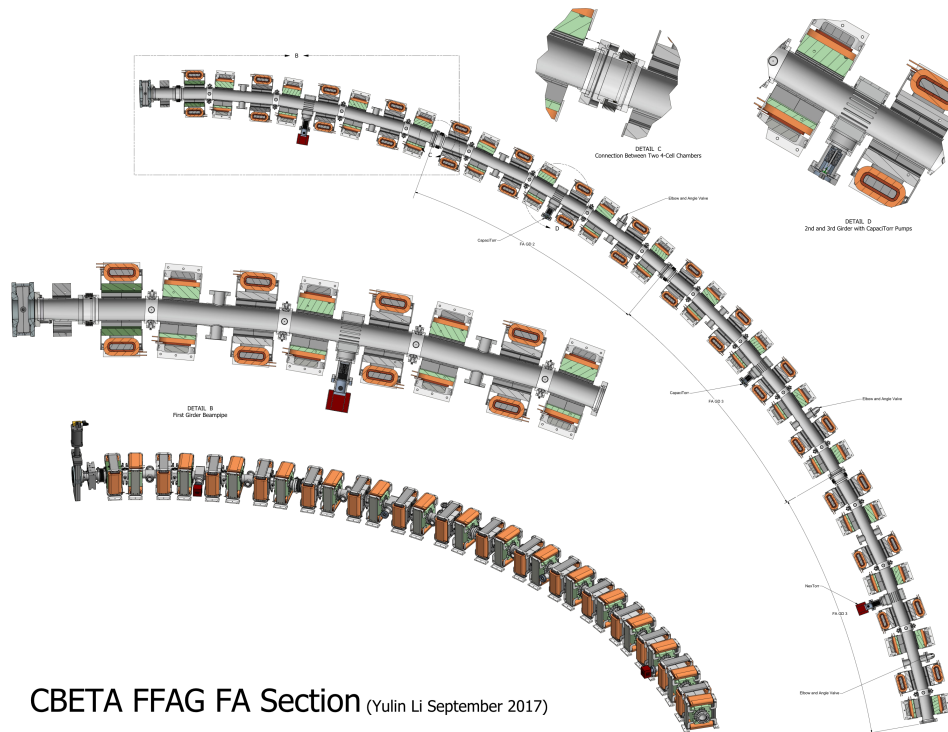


Figure 0.10.9: The FA arc shown in the horizontal projection and in the three dimensional case together with a single cell.

0.11 DRY-RUN plans - Virtual CBETA Machine results with errors

During the next couple of months in October, November and December 2018 a testing of the CBETA-V will be performed.

0.12 EPICS Control System Training

The EPICS control system training has started on Thursday September 6 and will continue through the next couple of months on Thursday's Accelerator physics meetings. Here are few titles from the first lecture and few illustrations:

External EPICS Reference Links

What is an EPICS record

Structure of an EPICS name

Getting/Setting a record

From the EPICS Terminal

From Matlab

From Python

Using EDM

Few illustrations from the first lecture shown bellow. The screen shown in Fig. 0.12.1 is related to the protection systems.

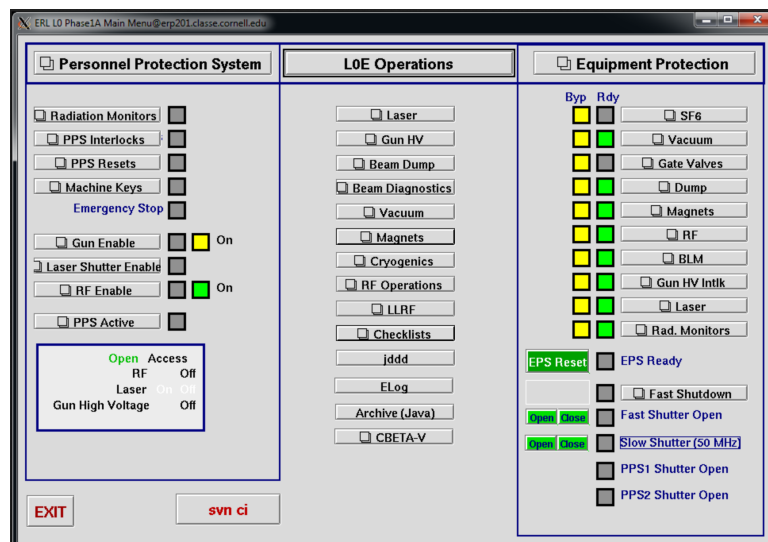


Figure 0.12.1: A screen from the EPICS control system related to the protection systems.

The screen shown in Fig. 0.12.2 shows control of the magnet currents.

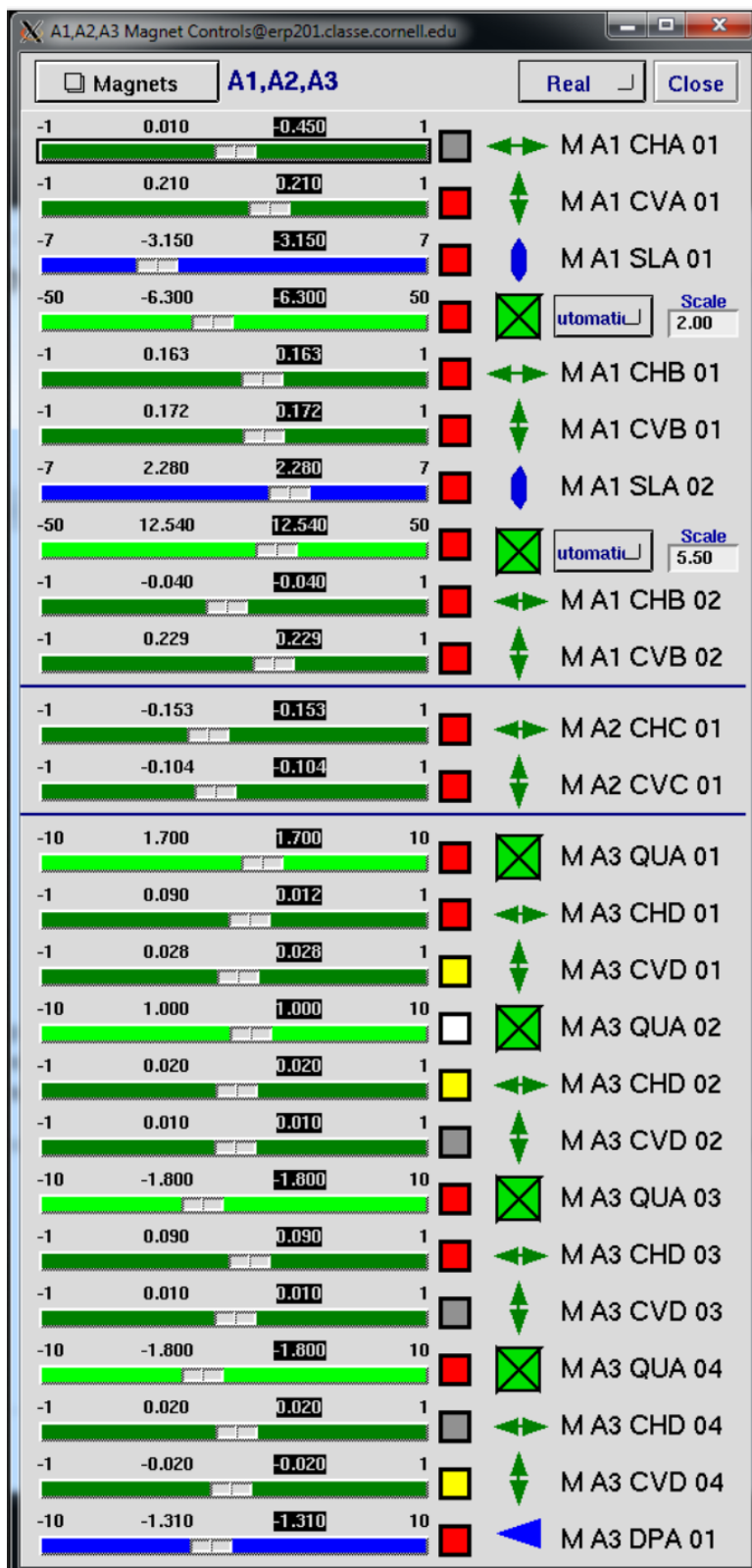


Figure 0.12.2: A screen from the EPICS control system related to the magnet strength control.

0.13 Software Routines-Scripts developments

The software script routines developed during the FAT commissioning continue to be developed not only by the Cornell physicists Adam Bartnik, Colwyn Gulliford, David Sagan, and William Lou, but as well as collaborators from UK and BNL.

0.14 FFA Correction magnet system

The FFA magnet orbit correction system is made of two types of the 'window frame' correctors: the vertical orbit corrector placed around the defocusing combined function permanent magnet and horizontal orbit corrector placed around the focusing permanent magnets are shown in Fig. 0.14.1.



Figure 0.14.1: A screen from the EPICS control system related to the magnet strength control.

0.15 Loss Monitor System

This part of the document is written by using John Dobbins presentation about the CBETA equipment protection - particularly Beam Loss Monitor system. There are main subjects of concern:

1. ERL Operation Interlocks
 - a) Personnel Protection Shutter
 - b) Equipment Protection Shutters
 - i. Inputs from Gun (SF6, High Voltage Power Supply)
 - ii. Inputs from Vacuum system - gate valves
 - iii. Inputs from Magnets and Magnet power supplies
 - iv. Inputs from the RF
 - v. Inputs from the slow radiation Monitors

- i. PPS
- ii. Equipment Protection system above
- iii. Gun, High voltage
- iv. Dump raster, Quad Detector, Temperature
- v. Beam Loss Monitors

The rest of information about the loss monitors is presented in the John Dobbins presentation.

0.16 Beam Position Monitors and time arrival monitors of the multi energy beams

There is additional document about the Beam Position Monitor system and Beam Arrival Monitor system written by Robert Michnoff.

0.17 Safety System and Review

The safety system is shown in our CBETA Design Report.

0.18 CBETA Beam commissioning plan

0.18.1 Concepts and Philosophy

An ERL is a non-equilibrium system that lacks a closed orbit and may not possess global transverse or longitudinal stability. Dynamically it is more closely related to time-of-flight spectrometers and injector systems than the conventional linear and circular accelerators that it superficially resembles. ERLs therefore encounter numerous unique operational challenges. Firstly, longitudinal motion dominates the dynamics: timing and energy control set the system architecture, and thus RF phase and gradient control must be assured, as must the lattice momentum compaction, the correlation of time of flight with energy. Secondly, the non-equilibrium nature of an ERL means that stability is a significant challenge. Thirdly, halo effects dominate high power operation (much as they do in injector chains); losses can be performance limiting: activation, damage (burn-through), and background for potential users are all issues. Finally, as inherently multi-pass systems, ERLs must control multiple beams with different properties (energy, emittance, position, phase) during transport through and handling in common beam line channels. Successful machine operation thus requires a comprehensive strategy for machine commissioning, monitoring machine health, system stabilization, and machine protection.

ERL operation comprises a series of phases: commissioning, beam operation, and machine tuning/recovery. During each phase, system behavior falls into various classes that can be differentiated by the time scales on which they are manifest: “DC” conditions, those associated with the machine set point, “drift” effects, slow wandering of the set-point (due to, for example, thermal effects) degrading system output, and “fast” effects (at acoustical to RF time scales), resulting in beam instabilities. A fourth class, that of transient effects (for example, RF

loading during beam on/off transitions and fast shut-down in the event of sudden beam loss for machine protection purposes), can occur throughout all operational cycles.

Machine commissioning has combined goals of validating system design architecture and defining a recoverable system operating point. For an ERL, this requires demonstration of the control of phenomena of concern such as BBU and the micro-bunching instability (μ BI), while generating settings for hardware components.

Following pre-commissioning “hot” checkout of accelerator components and testing of hardware subsystems, beam operations commence with threading of low power beam so as to establish a beam orbit and correct it to specified tolerances. At this stage, system performance is error dominated. Some errors (such as RF phases or magnet installation errors) can be readily detected and corrected; others are subliminal, below the resolution of diagnostics or individual measurements, and will accumulate. Thus, some corrections are local (eliminating the error) and others must be global (such as the compensation of cumulative errors).

This requires orbit correction systems based on beam position monitors and steerers (typically every quarter-betatron wavelength); unique to a multi-pass ERL with common transport of multiple beams in a single beam line is the requirement that the system correct perturbations locally so that the multiple passes respond identically and the orbits not diverge unacceptably from turn to turn. Similarly, a baseline for longitudinal beam control must be established, by synchronizing the beam to the RF using recirculator arcs as spectrometers for precision measurements of energy gain. Any path length adjustments needed to set RF phases and insure energy recovery per the design longitudinal match are thus determined.

With a 6-D phase space reference orbit thus defined, the beam and lattice behavior is tuned and validated. Lattice performance is measured, tuned, and certified using differential orbit/lattice transfer function measurements; these, too, will require pass-to-pass discrimination for beams in common transport. Both transverse and longitudinal measurements (using phase transfer function diagnostics are necessary for a full analysis of lattice behavior. Corrections must be applied to ‘rematch the beam to the lattice acceptance’ and bring both transverse (betatron motion/focusing) and longitudinal (timing/momentum compaction) motion into compliance with design (or to establish an alternative working point).

Certification of lattice performance allows analysis, tuning, and validation of beam parameters, and matching of the beam to the lattice. This requires measurements of both betatron (emittance, beam envelope functions) and longitudinal (bunch length/energy spread/emittance, phase/energy correlation) properties. If beam properties differ excessively from specification, matching of the beam to the lattice is performed using appropriate correction algorithms. As with orbit correction, perturbations will likely require local correction so as to avoid excessive pass-to-pass divergence of beam properties. Given a validated working point, beam power scaling is performed, with currents increased from tune-up levels to full power CW.

0.18.2 Goals and Overview

The basic goal of commissioning is to demonstrate reproducible/recoverable machine operation with specific performance parameters. Given the precedence of longitudinal dynamics in an ERL, this requires, at the highest level, the proper adjustment of linac phases and gradients and transport system momentum compactions to confirm that they are in compliance with

the design. Provision must therefore be made for measurement of time of flight and energy as a function of phase, with adequate resolution to set phases and calibrate RF gradients to the tolerances required for successful FFA operation. This must be done on a pass-by-pass basis, initially setting RF parameters, and meeting subsequent phasing requirements by adjusting turn-to-turn path lengths. This is an iterative process, in which an initial orbit is established (the beam is “threaded”), and the RF is phased to the available resolution. Performance assessments (for both machine and beam) are then used to evaluate if iteration is required (to improve steering, phasing, and beam quality, correct machine errors, or improve address beam physics effects) or if the commissioning process moves forward. Commissioning activities move forward until beam quality is sufficiently degraded that progress slows or stops, or losses exceed tolerances for safe system operation. Characterization and analysis procedures are then applied to determine if performance limitations are due to the linac, the transport system, or are rooted in beam dynamical effects. This will involve measurements of beam energy, timing (phase) and time of flight, beam properties, and lattice characterization (typically using differential orbit measurement). In the following sections, a more detailed list of tasks and goals will be presented. The commissioning is phased, and each section will explain exactly what part of the beam line has been built, which diagnostics are installed, and what the goals are for that particular phase.

0.18.3 Commissioning Flow

There are five phases of commissioning, ending with 1-pass energy recovery at 1 mA average beam current, satisfying the Key Performance Parameter (KPP). Further operation, including multiple-pass operation, will not be described here as it falls outside of the scope of this report. Each of the following five phases will be separately described in the following sections.

1. Gun-ICM-Dump Recommissioning
2. MLC and Diagnostic Line
3. Partial Arc Energy Scan
4. Full Arc Energy Scan
5. KPP: Single Pass Energy Recovery

0.18.4 Gun-Linac-Dump Recommissioning

The first phase of commissioning will occur right after the gun, SRF injector cryomodule (ICM), and high power beam dump have been reinstalled in their new location. Because prior operation of the Cornell injector occurred at a different location, incompatible with the full CBETA ring design, we were forced to disassemble the injector and rebuild it at its present location. As a result, the first goal is to recommission typical operation of the injector. Thus, the primary goal of this phase is to check each machine subsystem with beam, discover what problems are present, and fix them.

The injector has set records for both low emittance and high average current, and recovering machine settings for both of these is important, but somewhat incompatible with the short

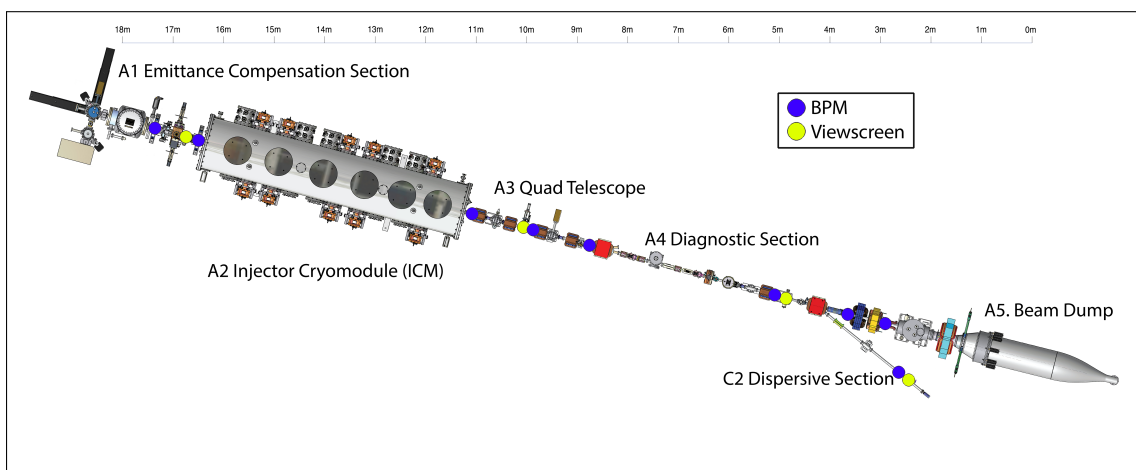


Figure 0.18.1: Beam line layout during gun-linac-dump recommissioning. BPMs and viewcreens are highlighted with blue and yellow circles, respectively.

timescale of this phase. As a result, beam emittance will not be measured, and we will focus on recommissioning the high current ability of the injector. So, we will forgo any detailed bunch diagnostics, and instead delay that until it can be done in the diagnostic line test, covered in the next commissioning section.

One of the largest advantages to this commissioning phase is the lack of the Main Linac Cryomodule (MLC). High current operation through the MLC requires full energy recovery, and thus a completed return loop to the linac. So, as soon as the MLC is installed, all high current operation is halted until the entire ring is complete. So, this phase of the project is both the first chance to test the gun and ICM at high current in the new location, and also the last chance to test it without a completed ring.

To that end, we will temporarily install a straight transport line after the ICM, identical to our previously tested design in the injector's prior location, and fully install the high power beam dump along with its water systems and radiation shielding. Both of these will be removed after this test, to allow installation of the merger, diagnostic line, and MLC. Diagnostics during this phase, as shown in Fig. 0.18.1, are limited to viewcreens and BPMs. All BPMs in this phase will have both position and phase information, using the same design as has been used in past injector operation. In addition, the high power beam stop also has two unique diagnostics, a quadrant current detector at its entrance, to detect small amounts of beam scraping, and an array of 8x10 thermocouples surrounding the dump, which give a rough position sensitivity to where and how the beam is hitting the dump. Both of these beam stop diagnostics will be tested during this phase. The rough procedure will be as follows.

Beginning with the setup of the gun and cathode system, two types of cathodes are required for operation, a large area cathode for initial alignment, and an small area off-center cathode for high current. At least three of each type will be produced. Initial operation will use a large (≈ 1 cm) active area photocathode, both to allow the laser to be aligned within the gun, and to reduce beam asymmetries inherent in off-center operation. These asymmetries do not affect machine performance, and can be easily tuned away later, but can confuse the initial beam alignment procedure, so it's useful to avoid them whenever possible.

After this, we would normally perform a somewhat lengthy alignment procedure for our initial low energy optics. Good alignment is only truly important when low emittance is desired, and that is not yet a requirement. So, without using the translation and angle adjustment motors on the solenoid magnets, a low duty factor beam will be centered as best as possible through the solenoids, while ignoring alignment in the buncher. Alignment in the first SRF cavity will be quickly adjusted and verified by ensuring the beam position downstream is not sensitive to variations of $\pm 10^\circ$ in cavity phase. The alignment in the additional downstream SRF cavities will not be checked and is not required.

SRF cavities will be individually set to 1 MeV energy gain, and phased on crest. This is not the intended CBETA operating point, and does not minimize the beam emittance, but is sufficient to test basic operation of the ICM at high current. There is no deflector installed, nor emittance measurement equipment, so the properties of the resulting bunch will not be studied in detail. Instead, the beam will be guided to the dump, and optics tuned as needed to minimize loss. When this is finished, the large active area cathode will be swapped out to an off-center small-area photocathode, appropriate for high current. Still with low duty cycle, the laser will be re-guided to the new location of the active area, and the electron beam orbit will be adjusted back to the previously set reference orbit.

Finally, the duty factor will be changed to 100%, and current will be increased by turning up the bunch charge. Of course, the properties of the bunch are changing as a function of charge, but since we have a short, straight beam line, the details of the bunch do not affect its ability to be transported successfully to the beam dump. The RF couplers into the SRF cavities will be set to their lowest current setting, since this requires the least amount of time for processing and setting up. With this setting, the klystrons will probably be unable to support beam currents higher than 5 mA, since almost all power will be reflected. But, this is sufficient to test our ability to reach the beam current requirements of the KPP, and any significant problems in high current operation can be addressed in this early phase of commissioning.

0.18.5 MLC and Diagnostic Line

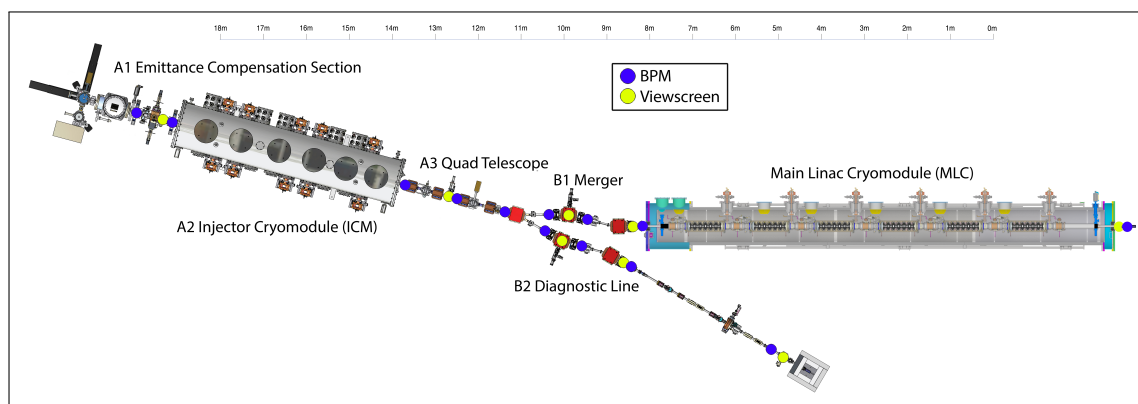


Figure 0.18.2: Beam line layout during MLC and diagnostic line commissioning. BPMs and viewcreens are highlighted with blue and yellow circles, respectively.

The next major commissioning phase is the MLC and diagnostic line test. The goal of this

test is to fully commission the injector to the intended CBETA operating point. This requires full characterization of the bunch at a variety of bunch charges in the diagnostic beam line, and demonstrated cavity-by-cavity acceleration in the MLC at the target cavity setpoint. At the end of the test, we should have a machine setpoint ready to be used for first pass operation of CBETA.

The diagnostics for this phase (Fig. 0.18.2) include the same position and phase BPMs used in the previous commissioning phase— that is, the switch to the new BPM electronics design has not yet been performed. But, importantly, one prototype of this new design will be installed at the end of the diagnostic line, along with the pipe and BPM button dimensions appropriate for use in the FFA arc. This phase will preset our first opportunity to test this design, and the location of this BPM right before a viewscreen will allow the design to be full calibrated, and its nonlinear position correction to be tested.

All bunch characterization will be done in the diagnostic line (B2), which is designed to be a mirror image of the merger line (B1) to the MLC, so if the magnets are put at identical setpoints, then the bunch should have nearly identical properties as in the actual CBETA arc. We will use our Emittance Measurement System (EMS), described elsewhere, to characterize both horizontal and vertical 2D phase spaces of the beam, the longitudinal current profile of the bunch. This allows us to know both the emittance and the twiss parameters of the bunch as it would have on entering the MLC. All of those parameters are critical to match into the rest of the CBETA arc, and are very difficult to predict in this low energy part of the machine where space charge still dominates the dynamics. After acceleration to 42 MeV, space charge is greatly suppressed, so having the full phase space knowledge of the beam is perhaps most important at this point. Importantly, this will also be the last point in the machine where the bunch can be fully characterized in this way.

We will adhere to the rule that at least three usable cathodes should be available at all times. To begin, a large area photocathode will be reinstalled into the gun, and the laser re-centered onto the photocathode. Now that low emittance will be required, alignment in the early low-energy beam line is crucial. The first week of commissioning will be spent aligning the solenoids with their motors, and the buncher and first two SRF cavities using dipole corrector magnets. The alignment procedure exists and has been used successfully multiple times in the past and will not be detailed here. Verification of the alignment is performed by checking beam emittance at $\ll 1$ pC bunch charge, at a charge where there is no emittance degradation from space charge. The emittance is measured in the diagnostic line, so this will be a good first test of the EMS. Once we demonstrate that this cathode emittance is preserved through the merger, it will be time to tune up the beam at non-trivial bunch charge.

Using the machine settings from simulation as a starting point, we will tune up the machine initially at 25 pC bunch charge. This is sufficient bunch charge to reach the Key Performance Parameter (KPP) of 1 mA with a bunch rate of $1300/31 = 41.9$ MHz, which is the maximum rate in the eRHIC bunch pattern mode of operation. Beam duty factor during this phase will be kept $\lesssim 0.1\%$, to minimize radiation, and indeed will be kept this low throughout all commissioning phases. The primary goal of the tune up is to reach a normalized emittance below $1\mu m$, as measured in the diagnostic line, while also matching desired beam twiss parameters needed to match optics in the CBETA lattice. The tuning of the machine will be primarily manual tuning, but guided by simulated predictions around the ideal setpoint in simulation. The capability to predict machine response already exists in our simulation and has been used

similarly in the past.

Once the setpoint at 25 pC is determined, we will explore methods to maintain this twiss match as a function of bunch charge. Simulations predict that at moderate bunch charges, below ≈ 75 pC, good twiss match can be maintained by adjusting only the laser spot size, buncher voltage, and first SRF cavity phase as a function of bunch charge, and we will attempt to verify this with the beam. If true, this would present a remarkably simple way to tune the machine for different bunch charges, and for high current operation, it might allow current to be ramped up by increasing bunch charge. Whether this simple method works or not, low-emittance and twiss-matching machine setpoints will be determined at a variety of bunch charges, including at least 0.7, 3, and 25 pC, allowing flexibility during future commissioning phases. 0.7 pC is sufficient to meet the KPP 1 mA current with a 1.3 GHz laser, while 3 pC is a rough minimum charge for reliable BPM measurements.

Using the 3 pC setpoint, the beam will be steered towards the Main Linac Cryomodule (MLC). Initially, the MLC will be left unpowered, and the beam steered through to the downstream BPM and viewscreen, which are the only diagnostics after the MLC. Additional diagnostics were prohibited during this phase, due to space conflicts with existing infrastructure. If a good twiss-match was achieved, as stated above, the beam should be able to be guided through the MLC without any loss, even without powering any MLC cavities.

After this, each MLC cavity will be individually powered, one-by-one, to the desired CBETA operating point. In simulation, the cavity phase can be adjusted by at least $\pm 60^\circ$ from on-crest without significant defocusing of the beam. We will phase each cavity on-crest by adjusting the cavity phase and monitoring the arrival time at the downstream BPM. With $0.1 \mu\text{A}$ of beam current, our BPMs are capable of measuring arrival time with an uncertainty of 0.3° of RF phase. With $\pm 60^\circ$ of RF phase adjustment in the cavity, we expect from 3 to 10 degrees of arrival phase change, depending on the distance of the cavity to the BPM (i.e. depending on which cavity we are phasing), which should be easily measurable. This should enable us to phase the cavity on-crest within $\approx 5^\circ$, which is sufficient for this phase of commissioning. Later, when the splitter is installed, further refinement of the phase can be performed by using the splitter as a spectrometer.

0.18.6 Full Arc Energy Scan

At this point, the entire FFA arc will have been completed, and the first pass splitter line on both sides of the arc completed and connected to the MLC (Fig. 0.18.3). The goals of this phase are identical to the partial arc energy scan, except now including the entire FFA arc. So, the effect of FFA magnet position errors and injection errors from the splitter will now be greatly magnified. So, the goals will be the same, but the needed precision in tuning will be much higher. Diagnostics in the FFA will generally follow the guidelines of one view-screen per FFA girder, and one BPM per cell. Importantly, only every other BPM will be wired to readout electronics, as shown in Fig. 0.18.3, with the possibility of swapping electronics or adding additional electronics at a later time. All of those BPMs will be position-only, capable of seeing potentially all 7 beams when in multi-pass configuration. A few of the BPMs in the unwired girder position will be used as Beam Arrival Monitors, as in Fig. 0.18.3, placed roughly at the beginning of each FFA section. Though only useful in the initial single-pass mode of operation, these BPMs will still be a valuable way to measure arrival phase separately

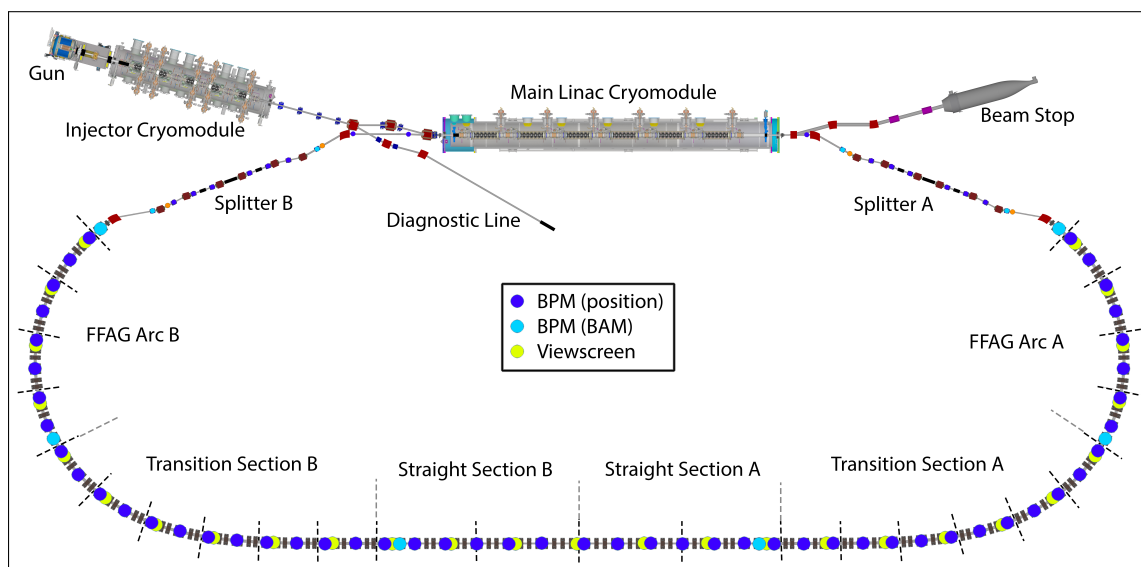


Figure 0.18.3: Beam line layout during full arc commissioning. The “flat pass” layout of the first splitter lines is shown, allowing energy recovery after a single pass.

at each of these parts of the arc. Diagnostic details of the second splitter, though not shown here, are identical to the details of the first splitter.

Beginning with the 42 MeV, 3 pC machine setting determined in the last phase, the beam will be progressively threaded through the rest of the FFA arc. This will likely be a long, iterative process. In each section of the FFA we will have the ability to compare to an online model of the ring, able to predict any needed corrector settings. In addition, the arc sections have the benefit that each cell should have the same orbit, and this periodicity will give us a simple way to check the beam’s behavior. Similarly, in the straight section the orbit is centered in the pipe, which is somewhat simpler conceptually, and perhaps easier in practice to tune. Also by virtue of the centered orbits, if the beam has the correct orbit, then the corrector magnets will have no effect on the orbit, which gives us an additional indirect orbit check at each magnet. The transition section orbit is likely to be the most challenging, since the orbit is neither periodic nor centered, so we will have to rely on comparisons to the model. Throughout this initial threading in the FFA, it is possible that only viewscreen and rough BPM measurements will be possible until the beam has been fully threaded through the arc, as the max operational current may be limited to prevent accidentally dosing and demagnetizing the permanent magnets. Beam loss monitors around the ring may prove to be a useful, though indirect, steering tool as the initial goal might be to simply minimize loss.

After successfully getting the beam through the FFA sections, and into the second splitter, the beam will be safely parked in the splitter’s first beam stop, in order to allow the current to be increased enough for higher precision BPM measurements. At this point, the orbit will be fine-tuned using the FFA corrector magnets, using the predicted magnet responses from simulation. The strengths needed to correct the orbit will give us information about any systematic problems with our FFA magnet installation, and depending on their severity, we will again evaluate the need to adjust the FFA magnet positions. Once a satisfactory orbit

has been achieved, difference orbits, dispersion, and arrival time measurements will be taken using each of the FFA correctors, at each of the available BPMs, and compared to model.

Finally, provided that the machine appears to be in its intended operating point, and the optics are verified to needed accuracy, we will once again slowly increase the energy of the MLC, while the splitter magnet strengths are similarly ramped up. The dependence of the orbit through the FFA will be checked against model in the same manner as in the partial arc test. This will be the final test of the acceptance of the FFA before future multiple-pass operation.

0.18.7 KPP: Single Pass Energy Recovery

This phase of commissioning occurs immediately after the previous phase, and no changes to the beam line or diagnostic layout will have been performed. At this point, the primary remaining difficulty is achieving energy recovery. The orbit through the second splitter will be threaded and then verified in the same manner as the first splitter, and then the beam will be guided into the MLC. If there is sufficient energy recovery for the beam to enter the dump beam line, then the path length for best energy recovery can be fine-tuned using the path length adjustment in both splitters. If either the adjustment range of the splitters is insufficient, or the path length is so inaccurate that the beam does not even enter the dump beam line, then more drastic changes will need to be made to the splitter beam lines, to add or subtract additional path length.

After the beam is successfully threaded into the dump, the next challenge is to raise the current. There are two strategies to do this: increase the number of bunches at a fixed charge, or increase the bunch charge at full duty factor. The first option requires the laser to achieve a large rejection ratio of laser pulses, so that the rejected part of the beam does not add up to a significant current. The rejected beam will be at a much smaller bunch charge than the desired part of the beam, and therefore be badly twiss-matched to the FFA lattice and likely be lost. This beam loss can be a potentially limiting source of radiation, and might make this approach impractical. However, the second option will require us to find a path in optics settings from zero to full bunch charge that preserves the lattice matching. If too many machine settings need to be varied, or if impractical changes to the initial laser properties are required, then this may also prove to be difficult. Both will have to be tested and evaluated.

Traditionally, the most difficult aspect of increasing the current is reducing the radiation from beam loss of the halo. Up until this phase of commissioning, we will not have had any direct way to measure the presence and effect of halo. The location of the beam loss will be known only indirectly by beam loss monitors, and simulation will have to be used as a guide for optics changes to reduce it. In past operation of our injector, problems with halo only became limiting when the beam current exceeded roughly 10 mA, and as such we may discover that the KPP current of 1 mA is below the threshold where it becomes important. But, due to the factor of 10 increase both in energy and length of the accelerator, compared to our previous experience, we cannot completely rely on that as a guide.

If it appears that using the eRHIC bunch pattern to reach the KPP current goal (i.e. 25 pC at 41.9 MHz) causes too many problems with halo, we can switch to a higher repetition rate laser and proportionally smaller bunch charge. We have an existing 1.3 GHz laser oscillator, which would offer the smallest possible bunch charge at the KPP 1 mA beam current. Using

the previously determined injector setting at 0.7 pC, we can still attempt to turn up the current to 1 mA. At such a small bunch charge, and at such a large bunch rate, the precision of the BPMs will be greatly reduced. So, in this mode of operation, if the optics need to be greatly adjusted, the laser would need to be temporarily switched back to the eRHIC rate in order to have accurate BPM readings. We have had two laser oscillators running simultaneously in the past, with the ability to quickly switch repetition rate, so this capability is possible.

In the end, regardless of the method used to reach 1 mA beam current, we will still attempt to raise the current as high as possible. That may require using an entirely new operating bunch charge, or potentially a similar switch to a high repetition rate laser to keep using the same bunch charge. Exploring the maximum usable current will be the final goal of this phase of operation.

0.19 Details of remaining installation and preparation for commissioning

The Table 0.19.1 shows the magnet counts for all FFA subsections in CBETA.

Table 0.19.1: Component count for FFA subsections. Corrector counts are for separated horizontal (H) and vertical (V) correctors.

subsection	Focusing (F) Quad	Defocusing (D) Quad	BPM	Corrector (H)	Corrector (V)
FA	16	17	16	16	16
TA	24	24	24	24	24
ZA+ZB	27	27	27	27	27
TB	24	24	24	12	12
FB	17	16	16	16	16
Total	108	108	107	107	107

The list of remaining items to be installed before the end of February is shown:

1. Details of remaining installation and preparation for commissioning
 - a) Finalize CBETA Installation before end of February
 - b) Receive (from the company KYMA), Measure, Correct, and Install all Fixed Field Halbach magnets 216 magnets on the 23 girders before the end of November and deliver them to Cornell after that.
 - c) Install the 23 girders in the Cornell hall LOE.
 - d) Survey the FFA magnets in November, December 2018, January 2019.
 - e) Receive (Sag Harbor Industries) all 216 correction magnets and install them together with Halbach magnets on the 23 girders.
 - f) Finish the production and commissioning of the BPM and BA electronic boards before the end of February 2019.

- g) Finish the production of septum and correction magnets at Cornell University before month of May 2019.
 - h) Receive (ELYTT-Bilbao Spain) and install all splitter magnets for the S1,S2, S3, S4 and R1, R2, R3, R4 beam lines before end of February. Missing magnets need to be at Cornell before month of May 2019.
 - i) Survey all splitter magnets before the end of February (missing elements before end of May 2019).
 - j) Receive the power supplies (SIGMA PHI France) for the fixed field correctors before November 2018 and test them and calibrate the correctors.
 - k) Receive the corrected RF circulators from SIGMA-PHI and install them in the MLC before December as there is a plan to have MLC up and running during December and January.
 - l) Order remaining the splitter magnet power supplies, receive and install before end of February for at least S1 and R1 splitter beam lines.
 - m) Install the vacuum system in the splitters and FFA arcs, transitions, and the straight section before end of January.
 - n) Install the shielding wall before end of December.
 - o) Install the water cooling system for the Halbach magnets (January 2019)
 - p) Order and receive the BPM cables before January 2019.
 - q) Install power supplies and BPM electronic racks.
 - r) Install the water cooling system for the splitter magnets.
2. Prepare and test the CBETA-V for the whole CBETA lattice.
 3. Finalize EPICS control with all the power supplies, BPMs beam arrival monitors names and dot the DRY-runs before end of February 2019.
 4. Use the results of the magnetic field measurements for the correct magnet transfer functions in EPICS control system.
 5. Prepare the scripts for orbit correction in the splitters and in the FA arcs.
 6. Test the corrections with the model using CBETA-V before end of February.
 7. Commission the new electron gun laser system before December 2018.
 8. Realign vertically the cavities in the MLC linac before December 2018.

A preparations for the fixed field magnet girder installation is in progress as shown in Fig.0.19.1 and Fig.0.19.2

The CBETA COMMISSIONING starts in March 1, 2019:

1. Recommission the S1 beam line with new common magnets.
2. Recommission the injector.

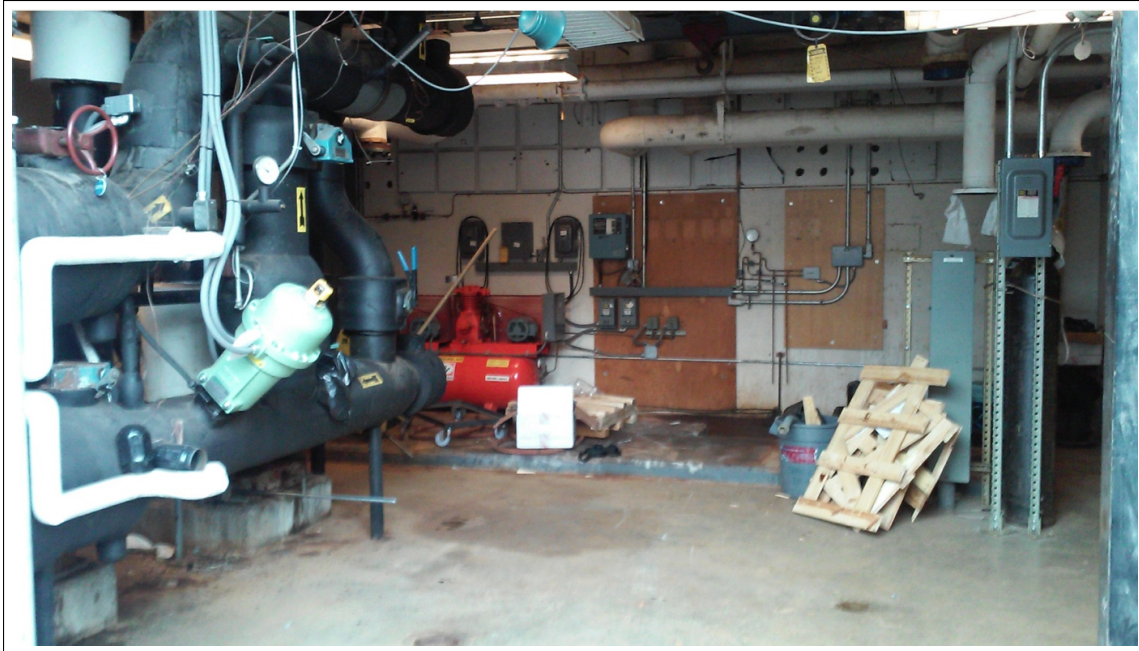


Figure 0.19.1: Preparation of the area for the FFA girder installation and cooling water supply.

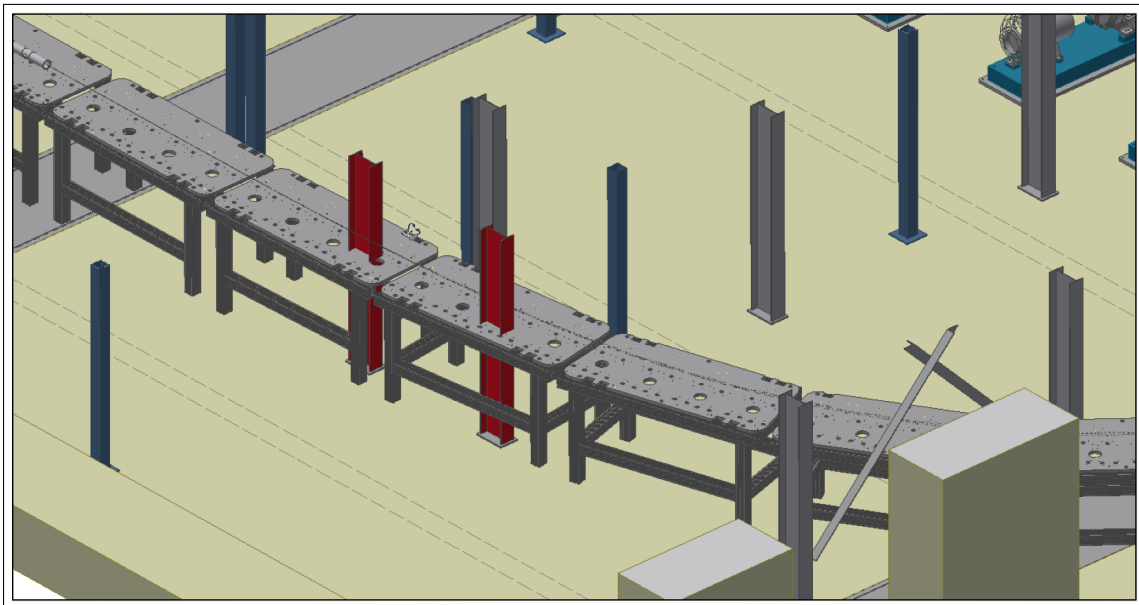


Figure 0.19.2: Area for the FFA arc girder installation. Few support poles need to be repositioned.

3. Recommission the MLC and redo the cavity phasing.
4. Match the S1 beam line to the FFA arc: dispersion and betatron functions.
5. Send the 42 MeV beam and correct the orbit through the first FFA arc FA and correct the orbit up to the TA transition.
6. Measure the betatron functions and the dispersion.
7. Continue the orbit correction through the transition TA.
8. Measure the dispersion and beam sizes.
9. Get the beam through the straight section ZA,ZM, and ZB and correct the orbit.
10. Continue the orbit correction through the transition TB up to the FFA arc FB.
11. Correct the orbit through the arc FB up to the splitter line R1. Measure dispersion and beam sizes.
12. Match the splitter line R1 to the FFA arc FB.
13. Measure the beam time of flight from MLC to the splitter line R1.
14. Commission the splitter line R1.
15. Measure the time of flight up to the MLC.
16. Start the energy scan from the MLC through the S1 beam line and measure the dispersion function and M56.
17. Measure the orbit response from MLC up to the end of R1.
18. Start the energy recovery run the beam through the MLC.
19. Reconfiguration of the S1 and R1 beam lines and installation of the remaining magnets in the S2, S3, S4 and R2, R3 and R4 beam lines (Month of May and June)
20. Multi-pass energy recovery commissioning starts in July 2019.

List of concerns from the Cornell side are:

1. CHESS Upgrade project does not release resources as predicted.
2. Town of Ithaca building permits, inspections, and CO.
3. Schedule add-ons and acceleration (no slack-time).
4. Vacuum chamber fabrication for RX and SX sections.
5. Assembly of RX and SX sections.
6. Radiation shielding (southeast).
7. Designs for electric, cooling and HVAC are late.
8. Process for issuing contracts for # 7 work (need fast-track).